

“DETECTION AND CLASSIFICATION OF TRANSMISSION LINE FAULTS USING STOCKWELL TRANSFORM AND ARTIFICIAL NEURAL NETWORK”

A

Project Report

Submitted in the partial fulfilment of the requirements

For the Degree of

Bachelor of Engineering

In

Electrical (Electronics & Power)

By

Mr. Chinmay Patil

Mr. Kaushal Dave

Mr. Pratik Hiralkar

Mr. Rahul Katore

Ms. Vaishnavi Bhalerao

Mr. Tejas Bhoiwad

Under the guidance of

Mr. R. K. Mankar



DEPARTMENT OF ELECTRICAL ENGINEERING

SHRI SANT GAJANAN MAHARAJ COLLEGE OF ENGINEERING

SHEGAON 444 203 M.S (INDIA)

Session: 2022-2023



DEPARTMENT OF ELECTRICAL ENGINEERING
SHRI SANT GAJANAN MAHARAJ COLLEGE OF ENGINEERING
SHEGAON 444 203 M.S (INDIA)

Session: 2022-2023

2022-23

CERTIFICATE

Certified that the project report entitled, "DETECTION AND CLASSIFICATION OF TRANSMISSION LINE FAULTS USING STOCKWELL TRANSFORM AND ARTIFICIAL NEURAL NETWORK" is a bonafied work done under my guidance by

Mr. Chinmay Patil

Mr. Kaushal Dave

Mr. Pratik Hiralkar

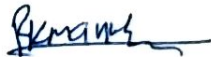
Mr. Rahul Katore

Ms. Vaishnavi Bhalerao


Mr. Tejas Bhoiwad

In partial fulfillment of the requirements for the award of degree of Bachelor of Engineering in Electrical (Electronics & Power).

Date: 15/5/2023


Mr. R. K. Mankar
Guide

Approved


(Dr. S. R. Paraskar)
Head
Department of Electrical Engg


(Dr. S. B. Somani)
Principal

E-mail: principal@ssgmce.ac.in

hod_elpo@ssgmce.ac.in

Phone No. 07265-252116, 252216

Fax No. 07265-252346, 253602

ACKNOWLEDGEMENT

We first pray to our divine source of inspiration “**Shri Sant Gajanan Maharaj**” whose blessings are always with us.

We express our deep gratitude to our Respected Director **Mr. Shrikantdada**

Patil for his kind blessings, encouragement and providing us such a good opportunity.

No words could be good enough to express our deep gratitude to our respected **Principal Dr. S. B. Somani** for his kind blessings, inspiration and providing us the necessary support.

We feel great pleasure in expressing our deepest sense of gratitude and sincere thanks for valuable guidance, extreme assistance and cooperation extended to us by our **Interna Guide MR.R.K. Mankar** in preceding the completion of the project.

We are equally indebted to **Dr. S. R. Paraskar (Head, Electrical Engineering Department)** for extending necessary help, providing facilities and time-to-time valuable guidance. We are especially thankful to Prof. R. S. Kankale & Dr. S. S. Jadhao for their valuable suggestions and inspiration time to time.

This acknowledgement would be incomplete without expressing our special thanks to MR.R.K. Mankar and Prof. R. S. Kankale for their support during the work.

Last but not least, we would like to thanks all the teaching, non-teaching staff members of the Electrical Engineering Department, our family members and colleagues those who helped us directly or indirectly for completing this task successfully.

Mr. Chinmay Patil

Mr. Kaushal Dave

Mr. Pratik Hiralkar

Mr. Rahul Katore

Ms. Vaishnavi Bhalerao

Mr. Tejas Bhoiwad

ABSTRACT

Transmission lines are an imperative element of modern power systems. Any faults in them can cause an undesirable interruption in the power supply. Precise analysis of these faults is important in order to ensure an incessant supply of power. For this purpose, fault detection and classification is needed to clear any such faults and re-establish the system to maintain its normal operation.

Power system protection and transmission line reliability, and fault analysis poses new technical challenges. Two Bus test system has been opted for conducting the studies. The multiple fault conditions have been obtained by changing fault inception angle and fault type like line to ground (LG) fault, double line (LL) fault, double line to ground (LLG) fault and three phase faults with the involvement of the ground (LLL) along with triple line to line fault (LLL). The proposed system has been simulated in PSCAD to capture voltage and current signal during normal and fault conditions. The captured voltage and current signals are analysed using Stockwell -Transform (ST) to extract list out features from it. A feature vector will be created by computing the statistical parameters to train and test the Artificial Neural Network (ANN) for classifying various types of faults on transmission line faults. The proposed approach can accurately detect and classify the fault on the transmission line.

CONTENTS

ACKNOWLEDGEMENT	i
ABSTRACT	li
CONTENTS	iii
LIST OF TABLES	v
LIST OF FIGURES	vii
ABBREVIATION	viii
CHAPTER 1	1
INTRODUCTION	2
CHAPTER 2	4
LITERATURE SURVEY	5
CHAPTER 3	8
POWER SYSTEM	9
3.1 Transfer of Power Between Active Sources	9
3.2 Power System Faults	11
3.2.1 Introduction	11
3.2.2 Open Circuit Faults	12
3.2.3 Short Circuit Faults	12
3.2.4 Causes of Faults	12
3.2.5 Consequences of Faults	13
3.2.6 Effect of Fault	14
3.2.7 Objectives of Short Circuit Analysis	14
3.2.8 Mathematical Modelling of LG Fault	14
CHAPTER 4	20
TRANSMISSION LINE	21
4.1 Introduction	21
4.2 Type of Transmission Line	21
4.2.1 Short Transmission Line	21

4.2.2 Medium Transmission Line	23
4.2.2.1 Nominal-T Representation	23
4.2.2.2 Nominal- Π Representation	24
4.2.3 Long Transmission Line - Rigorous Solution	25
CHAPTER 5	29
SIGNAL PROCESSING TECHNIQUES	30
5.1 Fourier Transform (FT)	30
5.2 Wavelet Transform (WT)	30
5.3 Stockwell Transform (ST)	31
5.4 Artificial Neural Network (ANN)	31
5.5 Limitation of Stockwell Transform, Fourier Transform, Wavelet Transform	32
5.6 The Sampling Theorem	32
CHAPTER 6	33
SIMULATION	34
6.1 PSCAD Introduction	35
6.1.1 PSCAD Applications	35
6.2 System UNDER STUDY	36
6.3 Simulation in PSCAD	36
6.4 Result Analysis in PSCAD	37
CHAPTER 7	39
PROPOSED METHODOLOGY	40
7.1 Workflow of System	41
CHAPTER 8	42
INTRODUCTIONS TO MATLAB	43
8.1 Application of MATLAB	43
CHAPTER 9	45
STOCKWELL TRANSFORM	46
9.1 Introduction	46
9.2 Need of S-Transform Approach	46

9.3 Fault Index	47
9.4 Feature Extraction By S-Transform	47
9.5 Proposed Flowchart of Stockwell transform	47
CHAPTER 10	50
S-TRANSFORM RESULT AND DISCUSSION	51
10.1 Phase to Ground (LG)Fault	51
10.2 Double Line (LL) Fault	52
10.3. Double Line to Ground (LLG)Fault	53
10.4. Three-Phase Line (LLL) Fault	55
10.5 Three-Phase Fault Involving Ground (LLLG)Fault	56
10.6 Fault Index Magnitude at Different Fault	57
CHAPTER 11	58
ARTIFICIAL NEURAL NETWORKS	58
11.1 Introduction	59
11.2 Architecture of ANN	59
11.3 Back Propagation Learning	60
11.4 Back Propagation Algorithm	61
11.5 ANN Design for Fault Classification	63
CHAPTER 12	64
Results and Discussion	65
CHAPTER 13	71
CONCLUSION	72
REFERENCES	73
APPENDIX	

LIST OF TABLES

3.1 Percentage of occurrence of fault on various power system equipment	13
3.2 Frequency occurrence of fault	14

10.1 Types of Faults and Magnitude	57
12.1 Energy values of current signals for LG faults	65
12.2 Energy values of current signals for LL faults	66
12.3: Energy values of current signals for LLG faults	66
12.4: Energy values of current signals for LLL faults	67
12.5: Energy values of current signals for LLLG faults	67
Generator Parameters	
Bus Voltages	
Transmission Line Parameters	

LIST OF FIGURES

3.1 Various types of faults occur on three-phase power transmission system	13
4.1 Equivalent circuit of short line	22
4.2 Medium line, localized load-end capacitance	23
4.3 Medium line, nominal-T representation	23
4.4 Medium line, nominal- π representation	24
4.5 Schematic diagram of a long line	25
6.1 PSCAD Screen	34
6.2 Single Line Diagram of Two Bus System	36
6.3 Two Bus system (without fault)	36
6.4 Two Bus system (with fault)	37
6.5 Line Voltage(kv) Vs Time Waveform (sec)	37
6.6 Line Current (kA) Vs Time Waveform (kA)	37
6.7 Line Current Vs Time Waveform during LG Fault on T. L.	38
6.8 Line Current Vs Time Waveform during LL Fault on T. L.	38
6.9 Line Current Vs Time Waveform during LLG Fault on T. L.	38
6.10 Line Current Vs Time Waveform during LLL Fault on T. L.	38
6.11 Line Current Vs Time Waveform during LLLG Fault on T. L.	38

7.1 project workflow	41
9.1 Flowchart of Stockwell Transform	49
10.1 Line Current Vs Time During LG Fault on T. L.	51
10.2 Fault index calculated using current waveform during LG fault.	52
10.3 Line Current Vs Time During LL Fault on T. L.	52
10.4. Fault index calculated using current waveform during LL fault.	53
10.5 Line Current Vs Time During LLG Fault on T. L.	54
10.6 Fault index calculated using current waveform during LLG fault	54
10.7 Line Current Vs Time During LLL Fault on T. L.	55
10.8 Fault index calculated using current waveform during LG fault.	55
10.9 Line Current Vs Time During LLLG Fault on T. L.	56
10.10 Fault index calculated using current waveform during LG fault.	57
11.1 ANN architecture	60
12.1. Training confusion matrix	68
12.2. Testing confusion matrix	69
12.3. Validation confusion matrix	69
12.4. Overall confusion matrix	70

ABBREVIATIONS

L-G	Line to Ground
L-L	Line to Line
LL-G	Double Line to Ground
LLL	Line -Line-Line
LLL-G	Line-Line Line-Ground
AC	Alternate Current
DC	Direct Current
mA	Milli Ampere
μ f	Microfarad

k Ω	Kilo Ohm
Amp	Ampere
z	Series Impedance/Unit Length/Phase
y	Shunt Admittance/Unit Length/Phase to Neutral
r	Resistance/Unit Length/Phase
L	Inductance/Unit Length/Phase
C	Capacitance/Unit Length/Phase to Neutral
Z	Total Series Impedance/Phase
FT	Fourier Transform
ST	Stockwell Transform
WT	Wavelet Transform
ANN	Artificial Neural Network
PSCAD	Power System Computer-Aided Design
MATLAB	Matrix Laboratory
DFT	Discrete Fourier Transform
DWT	Discrete Wavelet Transform
FRST	Fractional Stockwell Transform
FRFT	Fractional Fourier Transform
EMTDC	Electromagnetic Transients Including DC
FACTS	Flexible Alternating Current Transmission System
FIA	Fault Inception Angle
TL	Transmission Line
STFT	Short-time Fourier transform
E _{1a}	Energy of phase A
E _{1b}	Energy of phase B
E _{1c}	Energy of phase C



CHAPTER 1

INTRODUCTION

INTRODUCTION

Modern power systems are designed to operate efficiently to supply power on demand to various load centres with high reliability. The generating stations are often located at distant locations for economic, environmental and safety reasons. For example, it may be cheaper to locate a thermal power station at pithead instead of transporting coal to load centres. Hydropower is generally available in remote areas. Thus, a grid of transmission lines operating at high or extra high voltages is required to transmit power from the generating stations to the load centres. In addition to transmission lines that carry power from the sources to loads, modern power systems are also highly interconnected for economic reasons.

The rapid growth of electric power system over the past few decades has resulted in large increase of the number of transmission lines in operation. The transmission lines are exposed to different atmospheric conditions leading to occurrence of various types of faults like L-G, L-L, LL-G, LLL, and LLL-G also due to lightning, short circuits, faulty equipment's, mal-operation, human errors, overloading, and ageing of equipment's etc. There is no fault-free system, and it is neither practical nor economical to build a fault-free system. The actual magnitude of fault current depends on resistance to flow and varied impedance between the fault and the source of power supply. Total impedance comprises of fault resistance, resistance and reactance of line conductors, impedance of transformer, reactance of the circuit, and impedance of generating station. When the electrical power system is subjected to a short circuit fault, it is accompanied by flow of huge fault current which may damage of the connected equipment's and also create power quality problems. Therefore, accurate fault detection and classification are very important tasks in power system protection which can restore the power supply and also to maintain the system stability and improve the reliability of power system.

In this project, 'THE TWO BUS TEST SYTEM' is considered and it is simulated in PSCAD software. Various types of fault (like LG, LL, LLG, LLL & LLLG) with fault resistance 0.01ohm are created at middle of transmission line by varying fault inception angle (FIA) from 0° to 360° in steps of 30°. Line current signal are captured at the receiving end. Data obtained from PSCAD is exported in MATLAB to apply S-transform. To determine fault index obtained from ST matrix.

Fault index is useful to determine to detect the fault. ST matrix is normalised in the frequency domain and is given as input to ANN model. Thus transmission line fault classification has been obtained from the confusion matrix.



CHAPTER 2
LITERATURE SURVEY

LITERATURE SURVEY

There has been extensive research in fault detection, fault classification to maintain reliability of power system and security within a satisfactory level for improvement of the performance of digital protective relays, renovation of power industry, and stability of the power system.

Rafael Arranz et al created a method employing ST and ANN to find, categorise, and pinpoint defects. These methods are applied to data from transitory recovery. Several model configurations, varying inception angle, fault resistance, equivalent capacitance, and type of fault are all mentioned by the authors. Using ST analysis [1]

Based on wavelet correlation modes, H. A. Jimenez et al created a method to identify and localise faults in multi-terminal transmission lines. [2]

Discussed by Seongmin Heo et al Classification issues using neural networks are how fault detection and identification issues are formulated. The Tennessee Eastman (TE) process is subjected to this neural network classifiers' application. [3]

According to Mohammad Javad Dehghani, this paper compares two methods for analysing and visualising voltage distortions with time-varying amplitudes. The Discrete Wavelet Transform (DWT) and the S-Transform are among the methods. [4]

M. Jayabharata Reddy et al discussed the non-stationary transient fault signals' dynamic properties are captured via the wavelet transform employing wavelet MRA coefficients. To extract significant features from wavelet MRA coefficients and arrive at coherent judgments about fault location, fuzzy logic is used in conjunction with expert evaluation through a fuzzy inference system (FIS). [5]

R. N. Mahanty et al discussed the Comparative study of the performance of DFT and DWT techniques applied to the detection, classification, and location of transmission line faults. From the results presented DWT technique being a multi-resolution technique gives better results in case of fault classification and in case

of estimating the fault distances when more than one phase is involved in a fault. [6]

D. Das et al discussed the Comparative study of the performance of DFT and DWT techniques applied to the detection, classification, and location of transmission line faults. From the results presented DWT technique being a multi-resolution technique gives better results in the case of fault classification and in the case of estimating the fault distances when more than one phase is involved in a fault. [7]

I. W. C. Lee et al discussed that the S-transform is similar to the wavelet transform but with a phase correction. This property is used to obtain useful features of the nonstationary signals that make the pattern recognition much simpler in comparison to the wavelet multiresolution analysis. [8]

Anup Kumar, Himanshu Sharma, et al discussed how the Hybrid Fault Index, which is used to identify and categories Transmission Line Faults, is computed using the Stockwell Fault Index. [11]

Two techniques for defect identification and classification were discussed by K. Chen, C. Huang, et al feature extraction from input signals, and a functioning algorithm that leverages features and infers the outcome. Several strategies are applied based on these two sections. like the Wavelet Transform (WT), S-Transform (ST), Fast Fourier Transform (FFT), and statistical techniques. [12]

Data collecting, feature extraction, ANN training, ANN testing, fault classification, and performance evaluation were discussed by Santosh K. Padhy, Basanta K. Panigrahi, et al in order to classify transmission line faults using an artificial neural network. [13]

M. B. Hessine et al proposed an ANN-based-fault classifier technique based on input data of each phase currents and the zero-sequence current component (four pre-fault and four post-fault for each phase and zero-sequence currents components) instead of pre and post-phase voltages. Moreover, the time domain of the four samples was used instead of the commonly used FFT [14].

Banu et al developed a new fault location method for a transmission line. The method uses one ANN based on the Levenberg Marquardt optimization technique. However, fault detection and fault classification are not indicated in this research. However, the error of this method was still below 0.65 % [15]

Triangle network protection is proposed using a new method that combines S-transform and ANN for a transmission line, as discussed by H. Shu, Q. Wu, et al. A time series' time-frequency representation is produced via the S-transform. It blends an imaginary spectral with a frequency dependence in a singular way. As a result, the energy of current acquired by the S-transform is chosen in this research as the characteristic of the neural network. The neural network is then trained and tested to create a model for defect diagnosis. Numerous simulation studies have demonstrated the method's viability and effectiveness.[16]

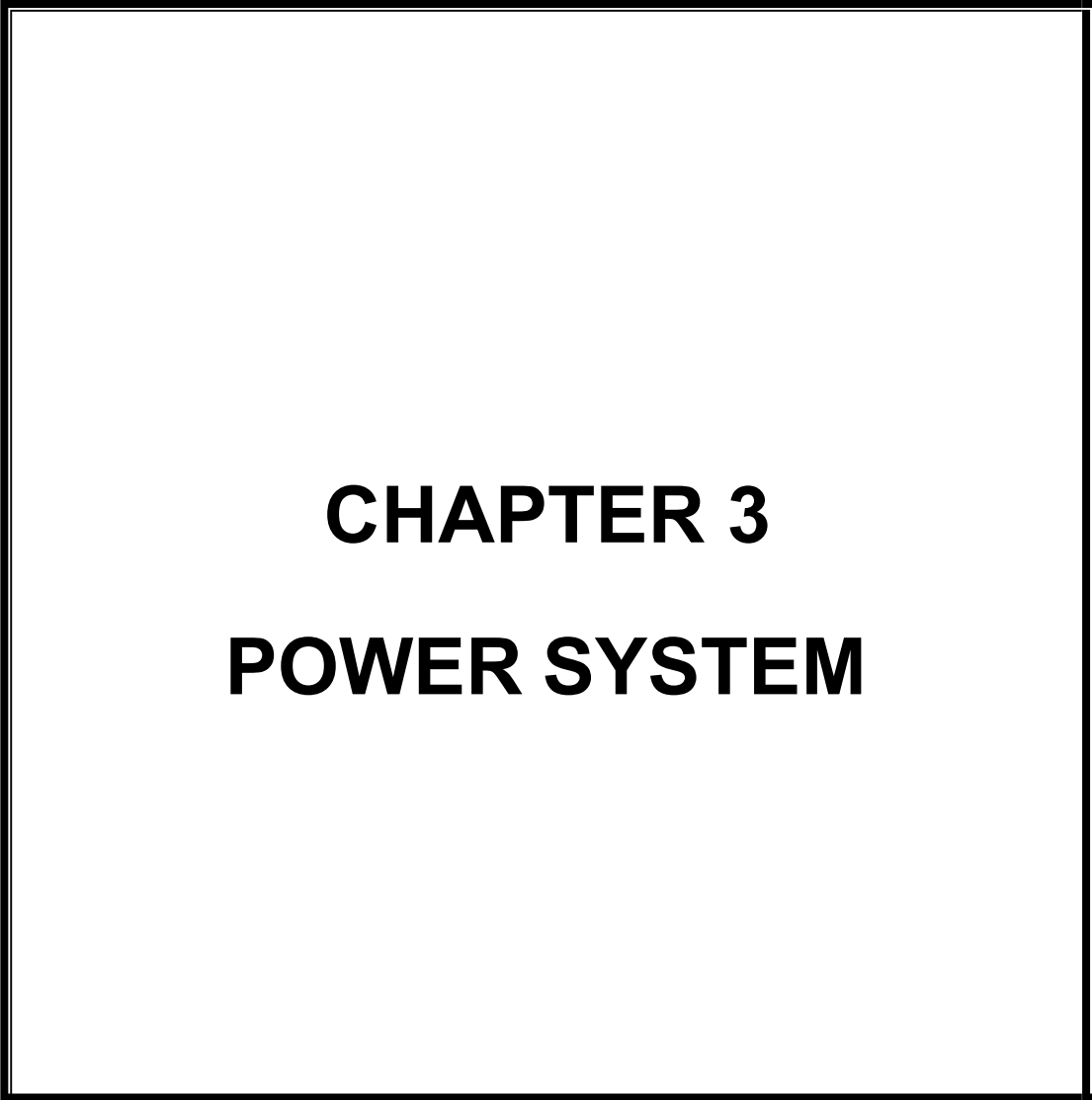
Project Objective

Objective 1: -

Transmission line faults detection using Stockwell Transform.

Objective 2: -

Transmission line faults classification using Artificial Neural Network.



CHAPTER 3
POWER SYSTEM

POWER SYSTEM

3.1. TRANSFER OF POWER BETWEEN ACTIVE SOURCES

The rapid growth of electric power system over the past few decades has resulted in large increase of the number of transmission lines in operation. The transmission lines are exposed to different atmospheric conditions leading to occurrence of faults due to lightning, short circuits, faulty equipment's, mal-operation, human errors, overloading, and ageing of equipment's etc. Modern power systems are designed to operate efficiently to supply power on demand to various load centres with high reliability. The generating stations are often located at distant locations for economic, environmental and safety reasons.

The parameters affecting the transmission of active and reactive power between two sources coupled by an inductive reactance will be discussed next. Such a system is representative of two sections of a power system interconnected by a transmission system, with power transfer from one section to the other.

A purely inductive reactance connecting the two sources has been taken into consideration. This is due to the mostly inductive nature of the impedances that characterise transmission lines, transformers, and generators. When the full network is represented by an appropriate model for each of its elements and then reduced to a two-bus system, the resulting impedance will be essentially an inductive reactance. The shunt capacitances of transmission lines do not explicitly appear in the model their effects are implicitly represented by the net reactive power transmitted. Analysis of transmission of active and reactive power through an inductive reactance thus gives useful insight into the characteristics of ac transmission systems.

$$\begin{aligned} \tilde{S}_R^* &= P_R + jQ_R = \tilde{E} \tilde{I} = \tilde{E}_R \left[\frac{\tilde{E}_S - \tilde{E}_R}{jX} \right]^* \\ &= \tilde{E}_R \left[\frac{E_S \cos \delta + jE_S \sin \delta - E_R}{jX} \right]^* \end{aligned} \quad (3.1. 1)$$

where,

\tilde{S}_R is the complex power at the receiving end (in VA)

P_R is the real power at the receiving end (in W)

Q_R is the reactive power at the receiving end (in VAR)

\tilde{E}_R is the voltage at the receiving end (in V)

\tilde{I}^* is the complex conjugate of the current at the receiving end (in A)

\tilde{E}_S is the voltage at the sending end (in V)

X is the inductive reactance (in Ω)

δ is the phase angle between the sending and receiving end voltages (in radians)

Hence,

$$P_R = \frac{E_S E_R}{X} \sin \delta \quad (3.1.2)$$

where,

P_R is the real power at the receiving end (in W)

$$Q_R = \frac{E_S E_R \cos \delta - E_R^2}{X} \quad (3.1.3)$$

where,

Q_R is the reactive power at the receiving end (in VAR)

Similarly,

$$Q_S = \frac{E_S^2 - E_S E_R \cos \delta}{X} \quad (3.1.4)$$

where,

Q_S is the reactive power at the sending end (in VAR)

describe the way in which active power and reactive power are transferred between active parts of a power network. Let us examine the dependence of active power and reactive power transfer on the source voltages by considering separately the effects of differences in voltage magnitudes and angles.

(a) We will look first at the condition with $\delta = 0$.

$$P_R = P_S = 0 \quad (3.1.5)$$

and,

$$Q_R = \frac{E_R(E_S - E_R)}{X} \quad (3.1.6)$$

$$Q_S = \frac{E_S(E_S - E_R)}{X} \quad (3.1.7)$$

The active power transfer is now zero. With $E_S > E_R$, Q_S and Q_R are positive, that is, reactive power is transferred from the sending end to the receiving end. The corresponding phasor diagram. With $E_S < E_R$, Q_S and Q_R are negative, indicating that reactive power flows from the receiving end to the sending end.

where,

Q_R is the reactive power at the receiving end (in VAR)

Q_S is the reactive power at the sending end (in VAR)

E_R is the voltage at the receiving end (in V)

E_S is the voltage at the sending end (in V)

3.2 POWER SYSTEM FAULTS

3.2.1 Introduction

A fault in an electrical device is described as a flaw in an electrical circuit that causes a current to flow in an unintended direction. Due to the low fault impedance, the fault currents are generally high. The three phases' voltages fall out of balance during the failures. Due to the large fault current, both the supply installation and the defective equipment may be harmed. Power flow is shifted toward the fault during faults, which also affects supply to the nearby zone. Voltage at the problematic point and overall impedance up to the fault location both affect the fault current's value. The voltage differs from its typical value at the fault location. The fault causes a continuous change in the voltage and current, and the resulting phenomena are known as transient phenomena. Transient is used to describe a fleeting event that happens for a brief time. Enhancing system design, equipment quality, and maintenance can reduce faults. It's impossible to eliminate errors.

3.2.2 Open circuit faults

Series Faults: Series faults, also known as open conductors, occur when the series impedance of the lines is unbalanced. These mistakes Faults that disrupt the symmetry in one or two phases are unbalanced faults.

3.2.3 Short circuit faults

1) Symmetrical Faults: Included in every phase (e.g., LLL, LLL-G). Known additionally as a solid or fastened defect. The system remains balanced and is referred to as having a symmetrical or balanced fault since all three phases are equally affected.

2) Unsymmetrical Faults: These can involve one, two, or more phases, with or without ground. (Examples: L-G, L-L, and LL-G). Unsymmetrical or unbalanced faults are those in which the network's balanced condition is interrupted.

- I. Single Location Faults: Common Shunt Faults.
- II. Multi-Location Faults: Cross-Country Faults.
- III. Evolving Faults: (EVFs): EVFs that can happen at different times throughout distinct phases of a fault at the same fault location.

The line patrolling crew may not be informed of the fault location and fault-phase since EVFs entail many fault inception instants.

3.2.4 Causes of faults

1) Symmetrical Fault: Symmetrical faults typically result from improper circuit breaker and earthing switch operation or synchronization. It happens when an earthing switch is unintentionally ON while a line is powered.

2) L-G fault, an asymmetrical fault It happens because of an insulator failure or flashover. The ground or neutral conductor is in contact with one conductor.

The L-L and LL-G fault is brought on by the swinging of two conductors, the shorting of wires by birds, kite strings, or tree limbs, or both. When two conductors hit the ground or meet the neutral conductor, an LL-G fault happens.

There is a good probability of a flashover or a power arc between the two conductors during monsoon season because the dielectric strength decreases.

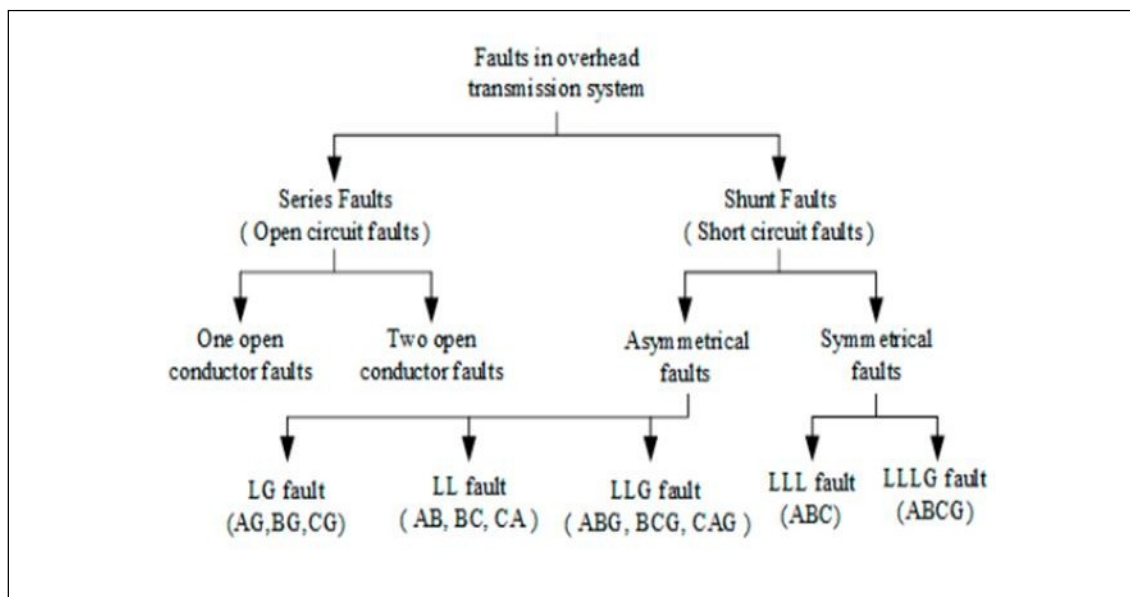


Fig 3.1 Various types of faults occur on three-phase power transmission system.

3.2.5 Consequences of faults.

Faults cause two types of damage.

- 1) Thermal damage: It happens gradually since it is temperature-related, i.e. the type of insulation. Thermal harm does not require instantaneous tripping.
- 2) Electrodynamic damage: The repelling forces produced by a big current would shape and structurally destroy the entire piece of equipment. Instantaneous tripping is necessary in the event of electrodynamic damage because the magnitude of the current is 10 to 20 times the entire load current.

Equipment	% of occurrence of Fault
Overhead transmission line	50
Underground Cable	10
Switchgear including CTs & PTs	15
Power Transformers	15
Miscellaneous	10

Table: - 3.1 Percentage of occurrence of a fault on various power system equipment

Type of Fault		% of occurrence of fault
Asymmetrical Fault	L-G	80 to 90 %
	L-L	6 to 10 %
	LLG	3 to 6 %
Symmetrical Fault	LLL/LLL-G	1 % or less

Table: -3.2 Frequency occurrence of fault

3.2.6 Effect of Fault.

- 1) Interruption in the power supply due to consumers.
- 2) Substantial loss of revenue due to interruption of service.
- 3) Loss of Synchronism: widespread blackout due to tripping of multiple lines / generators.
- 4) Extensive damage to equipment (transformers, generators, Induction Motors)
- 5) Serious hazards to personnel.

3.2.7 Objectives of Short Circuit Analysis / study or Fault calculations:

- 1) Design of power system and configuration of the network with considering the expected level of fault current.
- 2) Selection of interrupting capacity of the devices for operation on occurrence of fault and isolation of faulty equipment/subsystem from healthy part of the power system.
- 3) Selection of fault making rating of the interrupting devices when required to close against sustained fault.
- 4) Analysis of Performance of protective relays and their setting for proper their coordination.

3.2.8 Mathematical Modelling of (LG)Fault

The line to ground fault occurs at bus p (L-G) (or occurs to through Where z_F =Fault Impedance).

Self-impedance i.e., z_F^{aa} , z_F^{bb} i.e., Impedance between (a) to ground, (b) to ground and (c) to ground.

consider,

Fault in phase a through impedance. Fault impedance matrix ($z_F^{a,b,c}$) in terms of phase component.

$$[z_F^{a,b,c}] = \begin{bmatrix} z_F^{aa} & z_F^{ab} & z_F^{ac} \\ z_F^{ba} & z_F^{bb} & z_F^{bc} \\ z_F^{ca} & z_F^{cb} & z_F^{cc} \end{bmatrix} \quad (3.3.1)$$

Apply open circuit test Now calculate z_F^{aa}

Apply the 1pu current source at 'a' phase $I_a = 1pu$ measure the voltage at 'a' phase with respect to ground.

$$i. \quad [z_F^{aa}] = \frac{V_a}{I_a} = \frac{z_F \cdot I_a}{I_a} = \frac{z_F \cdot 1pu}{1 pu}$$

$$[Z_F^{aa}] = z_F \quad (3.3.2)$$

ii. Now, Z_F^{ab}

$$[z_F^{ab}] = \frac{V_b}{I_a} = \frac{-ZI_a}{I_a} = \frac{(0)1}{1} = 0$$

$$[z_F^{qb}] = 0 \quad (3.3.3)$$

iii. Now, Z_F^{ac}

$$[z_F^{ac}] = \frac{V_c}{I_a} = \frac{-ZI_a}{I_a} = \frac{(0)1}{1} = 0$$

$$[z_F^{qc}] = 0 \quad (3.3.4)$$

iv. Now, Z_F^{ba}

$$[z_F^{ba}] = \frac{V_a}{I_b} = \frac{-ZI_b}{I_b} = \frac{(0)1}{1} = 0$$

$$[Z_F^{ba}] = 0 \quad (3.3.5)$$

v. Now, Z_F^{bb}

$$[z_F^{bb}] = \frac{V_b}{I_b} = \frac{-ZI_b}{I_b} = \frac{(0)1}{1} = 0$$

$$[z_F^{pb}] = 0 \quad (3.3.6)$$

vi. Now, Z_F^{bc}

$$[Z_F^{bc}] = \frac{V_c}{I_b} = \frac{ZI_b}{I_b} = \frac{(0)1}{1} = 0$$

$$[Z_F^{bc}] = 0 \quad (3.3.7)$$

vii. Now, Z_F^{ca}

$$[Z_F^{ca}] = \frac{V_c}{I_c} = \frac{ZI_c}{I_c} = \frac{(0)1}{1} = 0$$

$$[Z_F^{ca}] = 0 \quad (3.3.8)$$

viii. Now, Z_F^{cb}

$$[Z_F^{cb}] = \frac{V_b}{I_c} = \frac{ZI_c}{I_c} = \frac{(0)1}{1} = 0$$

$$[Z_F^{cb}] = 0 \quad (3.3.9)$$

ix. Now, Z_F^{cc}

$$[Z_F^{cc}] = \frac{V_c}{I_c} = \frac{ZI_c}{I_c} = \frac{(0)1}{1} = 0$$

$$[Z_F^{cc}] = 0 \quad (3.3.10)$$

Hence,

$$[Z_F^{a,b,c}] = \begin{bmatrix} Z_F^{aa} & Z_F^{ab} & Z_F^{ac} \\ Z_F^{ba} & Z_F^{bb} & Z_F^{bc} \\ Z_F^{ca} & Z_F^{cb} & Z_F^{cc} \end{bmatrix}$$

$$[Z_F^{q,b,c}] = \begin{bmatrix} Z_F & 0 & 0 \\ 0 & \infty & 0 \\ 0 & 0 & \infty \end{bmatrix} \quad (3.3.11)$$

we will calculate $[Y_F^{a,b,c}]$ 3 phase Fault admittance matrix in terms of phase component.

$$[Y_F^{q,b,c}] = \begin{bmatrix} Y_F & 0 & 0 \\ 0 & 0 & 0 \\ 0 & 0 & 0 \end{bmatrix} \quad (3.3.12)$$

Now,

$$[Y_F^{a,b,c}] = [T_S^*][Y_F^{q,b,c}][T_S] \quad (3.3.13)$$

$$[Y_F^{0,1,2}] = \frac{1}{\sqrt{3}} \begin{bmatrix} 1 & 1 & 1 \\ 1 & a & a^2 \\ 1 & a^2 & a \end{bmatrix} \begin{bmatrix} y_F & 0 & 0 \\ 0 & 0 & 0 \\ 0 & 0 & 0 \end{bmatrix} \frac{1}{\sqrt{3}} \begin{bmatrix} 1 & 1 & 1 \\ 1 & a^2 & a \\ 1 & a & a^2 \end{bmatrix}$$

$$[Y_F^{0,1,2}] = \frac{1}{3} \begin{bmatrix} y_F & 0 & 0 \\ y_F & 0 & 0 \\ y_F & 0 & 0 \end{bmatrix} \begin{bmatrix} 1 & 1 & 1 \\ a^2 & a & a^2 \\ a & a^2 & 1 \end{bmatrix} \quad (3.3.14)$$

$$[Y_F^{0,1,2}] = \frac{1}{3} Y_F \begin{bmatrix} y_F & 0 & 0 & 1 & 1 & 1 \\ y_F & 0 & 0 & 1 & a^2 & a \\ y_F & 0 & 0 & 1 & a & a^2 \end{bmatrix} \begin{matrix} \\ \\ \\ 3 \times 3 \\ 3 \times 3 \end{matrix}$$

$$[Y_F^{0,1,2}] = \frac{Y_F}{3} \begin{bmatrix} 1 & 1 & 1 \\ 1 & 1 & 1 \end{bmatrix} \quad (3.3.15)$$

Now determine,

current at p^{th} bus in terms of symmetrical components

$$I_{p(F)}^{0,1,2} = Y_F^{0,1,2} \{ (U + Z_{pp}^{0,1,2} Y_F^{0,1,2})^{-1} E_{p(0)}^{0,1,2} \} \quad (3.3.16)$$

$$I_{p(F)}^{0,1,2} = \frac{Y_F}{3} \begin{bmatrix} 1 & 1 & 1 \\ 1 & 1 & 1 \\ 1 & 1 & 1 \end{bmatrix} \begin{matrix} F \\ \\ \\ \end{matrix} + \begin{matrix} Z^{(0)} & 0 & 0 \\ 0 & Z_{pp}^{(1)} & 0 \\ 0 & 0 & Z_{pp}^{(2)} \end{matrix} \begin{matrix} 1^{-1} \\ \\ \\ \end{matrix} \begin{bmatrix} 1 & 1 & 1 \\ 1 & 1 & 1 \\ 1 & 1 & 1 \end{bmatrix} \begin{matrix} 0 \\ [\sqrt{3}] \\ 0 \end{matrix}$$

where,

$$E_{p(0)}^{0,1,2} = \frac{1}{\sqrt{3}} \begin{bmatrix} 1 & 1 & 1 \\ 1 & a & a^2 \\ 1 & a^2 & a \end{bmatrix} [a^2] = \frac{1}{\sqrt{3}} \begin{bmatrix} 1 + a^2 + a \\ 1 + a^3 + a^3 \\ 1 + a^4 + a^2 \end{bmatrix}$$

$$1 + a + a^2 = 0, a^3 = 1, a^4 = a^3 = a = a$$

$$E_{p(0)}^{0,1,2} = \frac{1}{\sqrt{3}} [3] = [\sqrt{3}] \quad (3.3.17)$$

$$[Z_{pp}^{0,1,2} Y_F^{0,1,2}] = \begin{bmatrix} Z^{(0)} & 0 & 0 \\ 0 & Z_{pp}^{(1)} & 0 \\ 0 & 0 & Z_{pp}^{(2)} \end{bmatrix} \frac{1}{3} \begin{bmatrix} 1 & 1 & 1 \\ 1 & 1 & 1 \\ 1 & 1 & 1 \end{bmatrix}$$

$$= \frac{Y_F}{3} \begin{bmatrix} Z^{(0)} + 0 + 0 & Z^{(0)} + 0 + 0 & Z^{(0)} + 0 + 0 \\ Z_{pp}^{(1)} & Z_{pp}^{(1)} & Z_{pp}^{(1)} \\ Z_{pp}^{(2)} & Z_{pp}^{(2)} & Z_{pp}^{(2)} \end{bmatrix}$$

$$= \begin{bmatrix} \frac{Y_F}{3} Z_{pp}^{(0)} & \frac{Z_{pp}^{(0)} Y_F}{3} & \frac{Z_{pp}^{(0)} Y_F}{3} \\ Z_{pp}^{(1)} \frac{Y_F}{3} & Z_{pp}^{(1)} \frac{Y_F}{3} & Z_{pp}^{(1)} \frac{Y_F}{3} \\ Z_{pp}^{(2)} \frac{Y_F}{3} & Z_{pp}^{(2)} \frac{Y_F}{3} & Z_{pp}^{(2)} \frac{Y_F}{3} \end{bmatrix} \quad (3.3.18)$$

$$\begin{aligned}
I_{p(F)}^{0'1'2} &= \begin{bmatrix} 1 & 1 & 1 \\ 1 & 1 & 1 \\ Z_{pp} & Z_{pp} & Z_{pp} \end{bmatrix}^{-1} \begin{bmatrix} y_F Z_{pp}^{(0)} \\ Z_{pp}^{(1)} \frac{y_F}{3} \\ (2) \frac{y_F}{3} \end{bmatrix} + \begin{bmatrix} Z_{pp}^{(0)} y_F \\ Z_{pp}^{(1)} \frac{y_F}{3} \\ Z_{pp}^{(2)} \frac{y_F}{3} \end{bmatrix}^{-1} \begin{bmatrix} (0) y_F \\ (1) \frac{y_F}{3} \\ (2) \frac{y_F}{3} \end{bmatrix}^{-1} \begin{bmatrix} 1 \\ \sqrt{3} \\ 0 \end{bmatrix} \\
I_{p(F)}^{0'1'2} &= \frac{1}{Z_{pp}^{(0)} + 2Z_{pp}^{(1)} + 3Z_{pp}^{(2)}} \begin{bmatrix} 1 \\ 1 \\ 1 \end{bmatrix} \\
I_{p(F)}^0 &= \frac{1}{Z_{pp}^{(0)} + 2Z_{pp}^{(1)} + 3Z_{pp}^{(2)}} \begin{bmatrix} 1 \\ -1 \\ 1 \end{bmatrix} \\
I_{p(F)}^1 &= \frac{\sqrt{3}}{Z_{pp}^{(0)} + 2Z_{pp}^{(1)} + 3Z_{pp}^{(2)}} \begin{bmatrix} 1 \\ -1 \\ 1 \end{bmatrix} \\
I_{p(F)}^2 &= \frac{1}{Z_{pp}^{(0)} + 2Z_{pp}^{(1)} + 3Z_{pp}^{(2)}} \begin{bmatrix} 1 \\ -1 \\ 1 \end{bmatrix}
\end{aligned} \tag{3.3.19}$$

The phase a, b, c components of fault current at bus be obtain by primultiplying both sides by above equation Ts

$$\begin{aligned}
I_{p(F)}^a &= \frac{3I_{p(F)}^1}{Z_{pp}^{(0)} + 2Z_{pp}^{(1)} + 3Z_{pp}^{(2)}} \\
I_{p(F)}^b &= \begin{bmatrix} 1 & 0 \\ 0 & 1 \\ 0 & 0 \end{bmatrix} \\
I_{p(F)}^c &= \begin{bmatrix} 1 & 0 \\ 0 & 0 \end{bmatrix}
\end{aligned} \tag{3.3.21}$$

Voltage at P^{th} bus (Faulted bus)

$$E_{p(F)}^{0'1'2} = Y_F^{0,1,2} \{ (U + Z_{pp}^{0,1,2} Y_F^{0,1,2})^{-1} E_{p(0)}^{0'1'2} \} \tag{3.3.21}$$

$$E_{p(F)}^{0'1'2} = \begin{bmatrix} 1 & 1 & 1 \\ 1 & 1 & 1 \\ Z_{pp}^{(0)} & Z_{pp}^{(1)} & Z_{pp}^{(2)} \end{bmatrix}^{-1} \begin{bmatrix} 0 \\ 0 \\ 0 \end{bmatrix} + \begin{bmatrix} Z_{pp}^{(0)} & 0 & 0 \\ 0 & Z_{pp}^{(1)} & 0 \\ 0 & 0 & Z_{pp}^{(2)} \end{bmatrix}^{-1} \begin{bmatrix} y_F \\ \frac{y_F}{3} \\ \frac{y_F}{3} \end{bmatrix} \begin{bmatrix} 1 & 1 & 1 \\ 1 & 1 & 1 \\ 1 & 1 & 1 \end{bmatrix}^{-1} \begin{bmatrix} 0 \\ \sqrt{3} \\ 0 \end{bmatrix}$$

$$E_{p(F)}^{0'1'2} = \frac{1}{Z_{pp}^{(0)} + 2Z_{pp}^{(1)} + 3Z_{pp}^{(2)}} \begin{bmatrix} -Z_{pp}^{(0)} & 1 \\ Z_{pp}^{(0)} & -Z_{pp}^{(1)} \\ Z_{pp}^{(0)} & -Z_{pp}^{(1)} \end{bmatrix} \begin{bmatrix} 1 \\ 1 \\ 1 \end{bmatrix} \tag{3.3.22}$$

$$\begin{aligned}
E_{p(F)}^0 &= \frac{\sqrt{3}}{Z_{pp}^{(0)} + 2Z_{pp}^{(1)} + 3Z_{pp}^{(2)}} \begin{bmatrix} -Z_{pp}^{(0)} & 1 \\ Z_{pp}^{(0)} & -Z_{pp}^{(1)} \\ Z_{pp}^{(0)} & -Z_{pp}^{(1)} \end{bmatrix} \begin{bmatrix} 1 \\ 1 \\ 1 \end{bmatrix} \\
E_{p(F)}^1 &= \frac{\sqrt{3}}{Z_{pp}^{(0)} + 2Z_{pp}^{(1)} + 3Z_{pp}^{(2)}} \begin{bmatrix} -Z_{pp}^{(0)} & 1 \\ Z_{pp}^{(0)} & -Z_{pp}^{(1)} \\ Z_{pp}^{(0)} & -Z_{pp}^{(1)} \end{bmatrix} \begin{bmatrix} 1 \\ 1 \\ 1 \end{bmatrix} \\
E_{p(F)}^2 &= \frac{\sqrt{3}}{Z_{pp}^{(0)} + 2Z_{pp}^{(1)} + 3Z_{pp}^{(2)}} \begin{bmatrix} -Z_{pp}^{(0)} & 1 \\ Z_{pp}^{(0)} & -Z_{pp}^{(1)} \\ Z_{pp}^{(0)} & -Z_{pp}^{(1)} \end{bmatrix} \begin{bmatrix} 1 \\ 1 \\ 1 \end{bmatrix}
\end{aligned}$$

$$\begin{aligned}
E_{p(F)}^a &= E_{p(F)}^0 \\
E_{p(F)}^b &= E_{p(F)}^1 \\
E_{p(F)}^c &= E_{p(F)}^2
\end{aligned}$$

The phase component (a, b, c) of the voltage at p can be obtain primultiplying both side by above equation by Ts.

$$[E_{p(F)}] = \begin{bmatrix} E_{p(F)}^{(a)} \\ E_{p(F)}^{(b)} \\ E_{p(F)}^{(c)} \end{bmatrix} = \begin{bmatrix} 1 \\ a^2 - \frac{-Z_{pp}^{(0)} - Z_{pp}^{(1)}}{Z_{pp}^{(0)} + 2Z_{pp}^{(1)} + 3Z_F} \\ a - \frac{-Z_{pp}^{(0)} - Z_{pp}^{(1)}}{Z_{pp}^{(0)} + 2Z_{pp}^{(1)} + 3Z_F} \end{bmatrix} \quad (3.3.23)$$

The voltage at the buses other than P

$$E_{i(F)}^{0'1'2} = E_{i(0)}^{0'1'2} - Z_{i(F)}^{0,1,2} \left[\begin{matrix} 0,1,2 \\ F \end{matrix} \right] \left[\begin{matrix} 0,1,2 \\ pp \end{matrix} \right] \left[\begin{matrix} 0'1'2 \\ F \end{matrix} \right] E_{p(0)} \quad (3.3.24)$$

$$[E_{i(F)}] = \begin{bmatrix} E_{i(F)}^0 \\ E_{i(F)}^1 \\ E_{i(F)}^2 \end{bmatrix} = \begin{bmatrix} 0 & Z_{ip}^{(0)} & 0 & 0 \\ \sqrt{3} & 0 & Z_{ip}^{(1)} & 0 \\ 0 & 0 & 0 & Z_{ip}^{(2)} \end{bmatrix} E_{p(F)}^{0'1'2}$$

$$[E_{i(F)}] = \begin{bmatrix} E_{i(F)}^0 \\ E_{i(F)}^1 \\ E_{i(F)}^2 \end{bmatrix} = \begin{bmatrix} 0 \\ \sqrt{3} \\ 0 \end{bmatrix} - \frac{\sqrt{3}}{Z_{pp}^{(0)} + 2Z_{pp}^{(1)} + 3Z_F} \begin{bmatrix} Z_{ip}^{(0)} \\ Z_{ip}^{(1)} \\ Z_{ip}^{(2)} \end{bmatrix} \quad (3.3.25)$$

Now,

$$[E_{p(F)}] = \begin{bmatrix} E_{p(F)}^a \\ E_{p(F)}^b \\ E_{p(F)}^c \end{bmatrix} = \begin{bmatrix} E_{p(F)}^0 \\ E_{p(F)}^1 \\ E_{p(F)}^2 \end{bmatrix} \begin{bmatrix} 1 & 1 & 1 \\ a & a^2 & a \\ a^2 & a & 1 \end{bmatrix}$$

$$[E_{i(F)}] = \frac{1}{\sqrt{3}} \begin{bmatrix} 1 & 1 & 1 \\ 1 & a^2 & a \\ 1 & a & a^2 \end{bmatrix} [E_{i(F)}^1]$$

$$[E_{i(F)}] = \begin{bmatrix} E_{i(F)}^a \\ E_{i(F)}^b \\ E_{i(F)}^c \end{bmatrix} = \begin{bmatrix} 1 \\ a^2 \\ a \end{bmatrix} - \frac{1}{Z_{pp}^{(0)} + 2Z_{pp}^{(1)} + 3Z_F} \begin{bmatrix} Z_{ip}^{(0)} + 2Z_{ip}^{(1)} \\ Z_{ip}^{(0)} - Z_{ip}^{(1)} \\ Z_{ip}^{(0)} - Z_{ip}^{(1)} \end{bmatrix} \quad (1.3.26)$$



CHAPTER 4
TRANSMISSION LINE

TRANSMISSION LINE

4.1 INTRODUCTION

Transmission line is the long conductor with special design (bundled) to carry bulk amount of generated power at very high voltage from one station to another as per variation of the voltage level. Power transmission systems are supported by their transmission lines. Moving big blocks of electric energy over great distances is both technically and economically viable because to the presence of a well-established, high-capacity system of transmission lines. Alternating current (AC) or direct current (DC) electric transmission of bulk power can be carried out using aerial lines, underground cables, or compressed gas insulated lines. The great majority of powerlines in use today are three-phase ac aerial (overhead) lines, with air acting as the insulating medium around bare conductors.

Series resistance, series inductance, shunt capacitance, and shunt conductance are the four factors that define an electric transmission line. A transmission line's performance qualities rely on the parameters. Due to its impact on power transmission efficiency and voltage drop, inductance is the most important series component. The primary shunt component and a source of reactive power is capacitance. The size of the operating voltage affects how important the shunt capacitance parameter is since the megavars produced are proportional to the square of the line voltage. The transmission capacity is mostly affected by the transmission speed, making the series resistance and shunt conductance the least significant characteristics. The real power transmission loss, however, is entirely determined by the series resistance, therefore its presence must be considered. The resistive leakage current is accounted for by the shunt conductance.

4.2 TYPES OF TRANSMISSION LINE

4.2.1 Short Transmission Line

For short lines of length 100 km or less, the total 50 Hz shunt admittance ($j\omega Cl$) is small enough to be negligible resulting in the simple equivalent circuit.

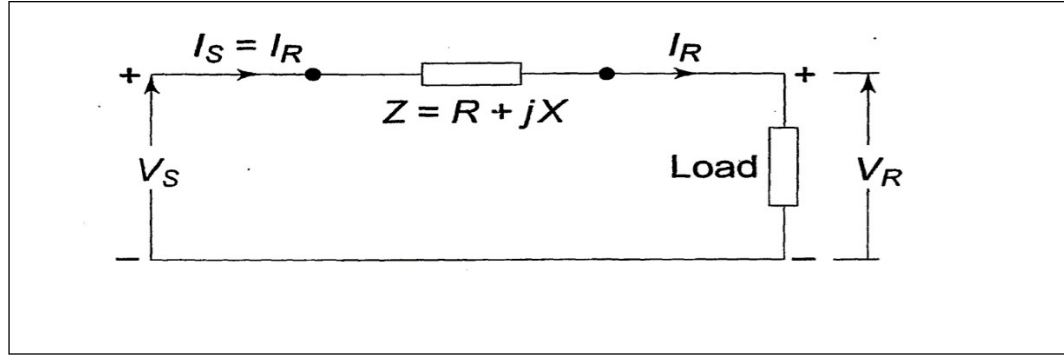


Fig 4.1: - Equivalent circuit of short line

This being a simple series circuit, the relationship between sending-end receiving-end voltages and currents can be written as:

$$\begin{bmatrix} V_S \\ I_S \end{bmatrix} = \begin{bmatrix} 1 & Z \\ 0 & 1 \end{bmatrix} \begin{bmatrix} V_R \\ I_R \end{bmatrix} \quad (4.2.1)$$

The phasor diagram for the short line is shown in Fig. 4.1 for the lagging current case. we can write.

$$|V_S| = [(|V_R| \cos \phi_R + |I|R)^2 + (|V_R| \sin \phi_R + |I|X)^2]^{1/2} \quad (4.2.2)$$

$$|V_S| = [|V_R|^2 + |I|^2(R^2 + X^2) + 2|V_R||I|(R \cos \phi_R + X \sin \phi_R)]^{1/2} \quad (4.2.3)$$

$$|V_S| = |V_R| \left[1 + \frac{2|I|R}{|V_R|} \cos \phi_R + \frac{2|I|X}{|V_R|} \sin \phi_R + \frac{|I|^2(R^2 + X^2)}{|V_R|^2} \right]^{1/2} \quad (4.2.4)$$

The last term is usually of negligible order,

$$\therefore |V_S| \cong |V_R| \left[1 + \frac{2|I|R}{|V_R|} \cos \phi_R + \frac{2|I|X}{|V_R|} \sin \phi_R \right]^{1/2} \quad (4.2.5)$$

Expanding binomially and retaining first order terms, we get

$$|V_S| \cong |V_R| \left[1 + \frac{|I|R}{|V_R|} \cos \phi_R + \frac{|I|X}{|V_R|} \sin \phi_R \right] \quad (4.2.6)$$

Or

$$|V_S| \cong |V_R| + |I|(R \cos \phi_R + X \sin \phi_R) \quad (4.2.7)$$

The above equation is quite accurate for the normal load range.

4.2.2 Medium Transmission Line

For lines more than 100 km long, charging currents due to shunt admittance cannot be neglected. For lines in range 100 km to 250 km length, it is sufficiently accurate to lump all the line admittance at the receiving-end resulting in the equivalent diagram shown in fig 4.4.

Starting from fundamental circuit equations, to write the transmission line equations in the $ABCD$ constant form given below:

$$\begin{bmatrix} V_S \\ I_S \end{bmatrix} = \begin{bmatrix} 1 + YZ & Z \\ Y & 1 \end{bmatrix} \begin{bmatrix} V_R \\ I_R \end{bmatrix} \quad (4.2.1)$$

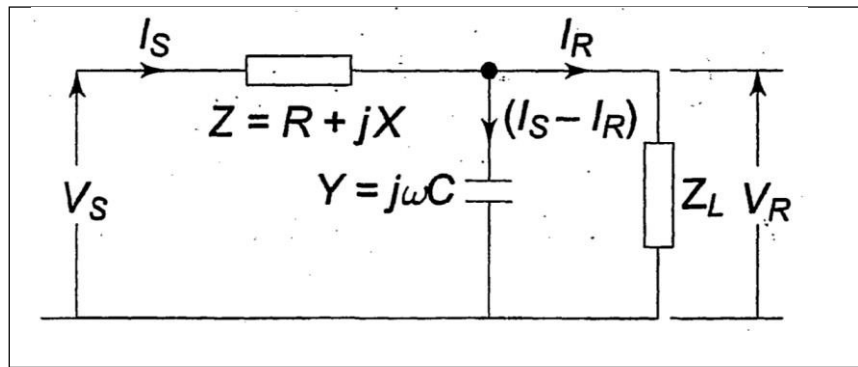


Fig 4.2: - Medium line, localized load-end capacitance

4.2.2.1 Nominal-T representation

If all the shunt capacitance is lumped at the middle of the line, it leads to the nominal-T circuit as shown in fig 4.5.

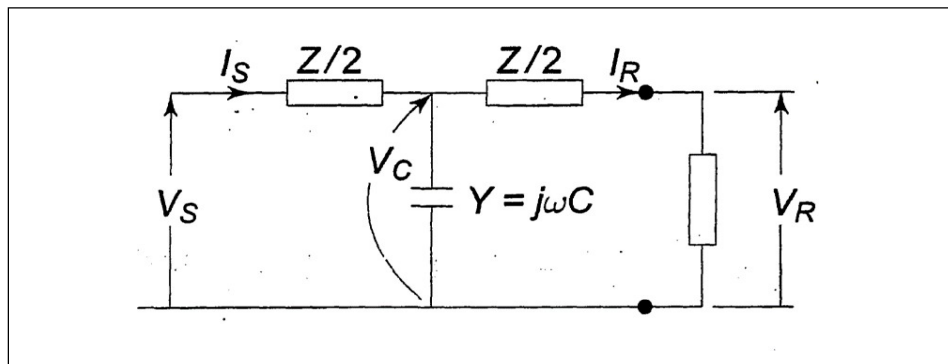


Fig 4.3: - Medium line, nominal-T representation

For the nominal-T circuit, the following circuit equations can be written:

$$V_C = V_R + I_R(Z/2) \quad (4.2.2.1.1)$$

$$I_S = I_R + V_C Y = I_R + Y V_R + I_R(z/2)Y \quad (4.2.2.1.2)$$

$$V_S = V_C + I_S(Z/2) \quad (4.2.2.1.3)$$

Substituting for V_C and I_S in the last equation, we get

$$V_S = V_R + I_R (Z/2) + (Z/2) [I_R + (1 + \frac{ZY}{2}) Y V_R] \quad (4.2.2.1.4)$$

$$= V_R (1 + \frac{ZY}{2}) + I_R Z (1 + \frac{YZ}{4}) \quad (4.2.2.1.5)$$

Rearranging, we get the following equations.

$$\begin{bmatrix} V_S \\ I_S \end{bmatrix} = \begin{bmatrix} (1 + \frac{1}{2}ZY) & Z(1 + \frac{1}{4}YZ) \\ Y & (1 + \frac{1}{2}YZ) \end{bmatrix} \begin{bmatrix} V_R \\ I_R \end{bmatrix} \quad (4.2.2.1.6)$$

4.2.2.2 Nominal- π representation

In this method the total line capacitance is divided into two equal parts which are lumped at the sending- and receiving-ends resulting in the nominal- π representation.

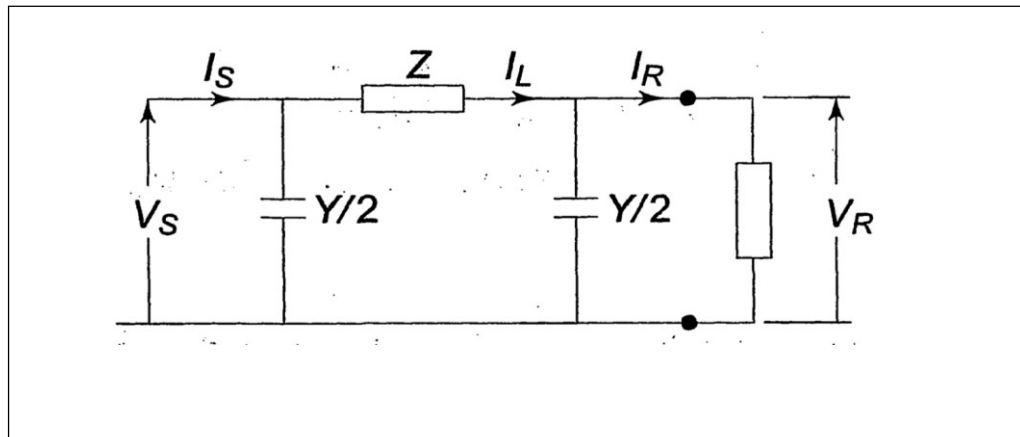


Fig 4.4: - Medium line, nominal- π representation

We have,

$$I_S = I_R + \frac{1}{2} V_R Y + \frac{1}{2} V_S Y \quad (4.2.2.2.1)$$

$$V_S = V_R + (I_R + \frac{1}{2} V_R Y) Z = V_R (1 + \frac{1}{2} YZ) + I_R Z \quad (4.2.2.2.2)$$

$$I_S = I_R + \frac{1}{2}V_R Y + \frac{1}{2}Y [V_R (1 + \frac{1}{2}YZ) + I_R Z] \quad (4.2.2.2.3)$$

$$I_S = V_R Y (1 + \frac{1}{4}YZ) + I_R (1 + \frac{1}{2}YZ) \quad (4.2.2.2.4)$$

Finally, we have

$$[I_S] = \begin{bmatrix} (1 + \frac{1}{2}YZ) & Z \\ Y(1 + \frac{1}{4}YZ) & (1 + \frac{1}{2}YZ) \end{bmatrix} [I_R] \quad (4.2.2.2.5)$$

It should be noted that nominal- T and nominal- π with the above constants are not equivalent to each other. The reader should verify this fact by applying star- delta transformation to either one.

4.3 LONG TRANSMISSION LINE - RIGOROUS SOLUTION

For lines over 250 km, the fact that the parameters of a line are not lumped but distributed uniformly throughout its length, must be considered.

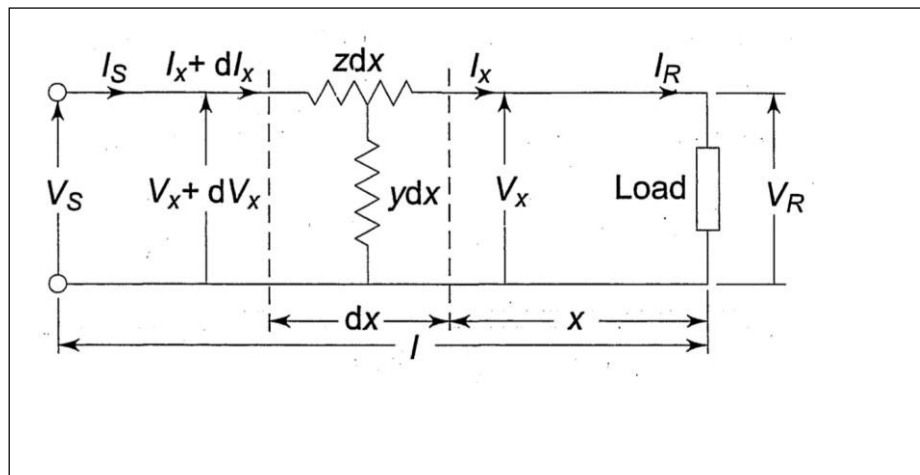


Fig 4.5: - Schematic diagram of a long line

one phase and the neutral return (of zero impedance) of a transmission line. Let dx be an elemental section of the line at a distance x from the receiving-end having a series impedance $z dx$ and a shunt admittance $y dx$. The rise in voltage to neutral over the elemental section in the direction of increasing x is dV_x . We can write the following differential relationships across the elemental section.

$$dV_x = I_x z dx \text{ or } \frac{dV_x}{dx} = z I_x \quad (4.3.1)$$

$$dI_x = V_x y dx \text{ Or } \frac{dI_x}{dx} = y V_x \quad (4.3.2)$$

It may be noticed that the kind of connection (e.g., T or π) assumed for the elemental section, does not affect these first order differential relations.

Differentiating Eq. (4.3.1) with respect to x , we obtain

$$\frac{d^2 V_x}{dx^2} = \frac{dI_x}{dx} z \quad (4.3.3)$$

Substituting the value of $\frac{dI_x}{dx}$ from Eq. (4.3.2), we get

$$\frac{d^2 V_x}{dx^2} = y z V_x \quad (4.3.4)$$

This is a linear differential equation whose general solution can be written as follows.

$$V_x = C_1 e^{\gamma x} + C_2 e^{-\gamma x} \quad (4.3.5)$$

where,

$$\gamma = \sqrt{y z} \quad (4.3.6)$$

and C_1 and C_2 are arbitrary constants to be evaluated.

Differentiating Eq. (4.3.5) with respect to x .

$$\frac{dV_x}{dx} = C_1 \gamma e^{\gamma x} - C_2 \gamma e^{-\gamma x} = z I_x \quad (4.3.7)$$

$$\therefore I_x = \frac{C_1}{z} e^{\gamma x} - \frac{C_2}{z} e^{-\gamma x} \quad (4.3.8)$$

where,

$$z = \left(\frac{z}{y}\right)^{1/2} \quad (4.3.9)$$

The constants C_1 and C_2 may be evaluated by using the end conditions, i.e., when $x = 0$, $V_x = V_R$ and $I_x = I_R$. Substituting these values in Eq. (4.3.5) and (4.3.8) gives

$$V_R = C_1 + C_2 \quad (4.3.10)$$

$$I_R = \frac{1}{Z_c} (C_1 + C_2) \quad (4.3.11)$$

which upon solving yield

$$C_1 = \frac{1}{2} (V_R + Z_c I_R) \quad (4.3.12)$$

$$C_2 = \frac{1}{2} (V_R - Z_c I_R) \quad (4.3.13)$$

With C_1 and C_2 as determined above, Eqs. (4.3.5) and (4.3.8) yield the solution for V_x and I_x as

$$V_x = \left(\frac{V_R + Z_c I_R}{2} \right) e^{\gamma x} + \left(\frac{V_R - Z_c I_R}{2} \right) e^{-\gamma x} \quad (4.3.14)$$

$$I_x = \left(\frac{V_R / Z_c + I_R}{2} \right) e^{\gamma x} - \left(\frac{V_R / Z_c - I_R}{2} \right) e^{-\gamma x} \quad (4.3.15)$$

Here Z_c is called the characteristic impedance of the line and γ is called the propagation constant.

Knowing V_R , I_R and the parameters of the line, using Eq. (4.3.13) complex number rms values of V_x and I_x at any distance x along the line can be easily found out. A more convenient form of expression for voltage and current is obtained by introducing hyperbolic functions. Rearranging Eq. (4.3.13).

we get,

$$V_x = V_R \left(\frac{e^{\gamma x} + e^{-\gamma x}}{2} \right) + I_R Z_c \left(\frac{e^{\gamma x} - e^{-\gamma x}}{2} \right) \quad (4.3.16)$$

$$I_x = \frac{1}{Z_c} \left(\frac{e^{\gamma x} - e^{-\gamma x}}{2} \right) + I_R \left(\frac{e^{\gamma x} + e^{-\gamma x}}{2} \right) \quad (4.3.17)$$

These can be rewritten after introducing hyperbolic functions, as

$$V_x = V_R \cosh \gamma x + I_R Z_c \sinh \gamma x \quad (4.3.18)$$

$$I_x = \frac{1}{Z_c} \sinh \gamma x + I_R \cosh \gamma x \quad (4.3.19)$$

When $x = l$, $V_x = V_S$, $I_x = I_S$

$$\therefore \begin{bmatrix} V_S \\ I_S \end{bmatrix} = \begin{bmatrix} \cosh \gamma l & Z_c \sinh \gamma l \\ \sinh \gamma l & \cosh \gamma l \end{bmatrix} \begin{bmatrix} V_R \\ I_R \end{bmatrix} \quad (4.3.20)$$

Here

$$A = D = \cos h \gamma l$$

$$B = Z_c \sin h \gamma l$$

$$C = \frac{1}{Z_c} \sin h \gamma l$$

In case $[V_S I_S]$ is known, $[V_R I_R]$ can be easily found by inverting Eq. (4.3.18). Thus

$$\begin{bmatrix} V_S \\ I_S \end{bmatrix} = \begin{bmatrix} D & B \\ -C & A \end{bmatrix} \begin{bmatrix} V_S \\ I_S \end{bmatrix} \quad (4.3.21)$$

CHAPTER 5

SIGNAL PROCESSING

TECHNIQUES

SIGNAL PROCESSING TECHNIQUES

5.1 FOURIER TRANSFORM (FT)

A Fourier transform (FT) is a mathematical transform that decomposes functions into frequency components, which are represented by the output of the transform as a function of frequency. Most commonly functions of time or space are transformed, which will output a function depending on temporal frequency or spatial frequency respectively. That process is also called analysis. An example application would be decomposing the waveform of a musical chord into terms of the intensity of its constituent pitches. The term Fourier transform refers to both the frequency domain representation and the mathematical operation that associates the frequency domain representation to a function of space or time. A Fourier transform (FT) is a mathematical transform that decomposes functions into frequency components, which are represented by the output of the transform as a function of frequency. Most commonly functions of time or space are transformed, which will output a function depending on temporal frequency or spatial frequency respectively. That process is also called analysis.

5.2 WAVELET TRANSFORM (WT)

Wavelet analysis deals with expansion of functions in terms of set of basic functions, like Fourier analysis, However, wavelet analysis expands functions not in terms of trigonometric polynomials but in terms of wavelets which are generated in the form of translations and dilations of a fixed functions called the Mother wavelet Compared with Fourier transform, wavelet can obtain both time and frequency information of signal, while only frequency information can be obtained by Fourier Transform

The sine waves and cosine waves are very smooth and are predictable whereas the wavelets are not smooth and are unpredictable, so wavelets are more suitable tool for studying the local behaviour such as spikes or discontinuity present in any signal. There are well defined families of standard wavelet, and we have also freedom of defining our own wavelet according to our requirement.

5.3 STOCKWELL TRANSFORM (ST)

Traditionally, the Fourier transform has been extensively used for analyzing the frequency contents of the signals. Besides, the FT is not an efficient analyzing tool for extracting the transient information of the non-stationary signals. Although the STFT divides the full-time interval into several small/equal-time intervals, can partly alleviate the problem, the STFT still has the limitation of a fixed window width. It is difficult to detect the occurrence times for very short duration and high-frequency signals. In order to avoid the disadvantages of both FT and STFT, the Wavelet Transform has been widely used for analysing the power quality problems.

The WT approach prepares a window that automatically adjusts to give proper resolutions of both the time and the frequency. In the approach, a larger resolution of time is provided to high-frequency components of a signal, and a larger resolution of frequency to low-frequency components. These features make the WT well suited for the analysis of the power system transients caused by various disturbances.

5.4 ARTIFICIAL NEURAL NETWORK (ANN)

Artificial neural network (ANN) can be applied to fault detection and classification effectively because it is a programming technique, capable to solve the nonlinear problems easily. The problems in which the information available is and in massive form can be dealt with. Also, the ANNs are able to learn with experiences, i.e., by the examples (Chaturvedi 2008).

The algorithm which employed ANNs programming offers many advantages, but it also suffers with many disadvantages, which are very complex in nature. Some of the important factors are the selection of type of network, architecture of the network (which includes the selection of number of layers, number of neurons in each layer, selection of activation functions, learning algorithms parameters etc.), termination criteria etc.

5.5 LIMITATION OF STOCKWELL TRANSFORM, FOURIER TRANSFORM, WAVELET TRANSFORM

- The continuous wavelet transform suffers from two drawbacks: redundancy and impracticality. The first is obvious from the nature of the wavelet transform and the second from the fact that both transform parameters are continuous.
- A major disadvantage of the Fourier Transform is it captures global frequency information, meaning frequencies that persist over an entire signal. This kind of signal decomposition may not serve all applications well (e.g. Electrocardiography (ECG) where signals have short intervals of characteristic oscillation).
- S-Transform are that it can observe how the frequency of the signal changes with time and has a straightforward interpretability of the results. Furthermore, it provides multi-resolution analysis while retaining the absolute phase of each frequency.
- ANN arms hanging along with the execution of parallel processing, and so they need processors that support parallel processing, so the ANNs are dependent on the hardware.

5.6 THE SAMPLING THEOREM

Statement: If the highest frequency contained in an analog signal $x_u(t)$ is $F_{\max} = B$ and the signal is sampled at a rate $F_s > 2F_{\max} \equiv 2B$. then $x_a(t)$ can be exactly recovered from its sample values using the interpolation function.

where,

F_{\max} represents the highest frequency component in the signal $x(t)$

F_s represents the sampling rate.

B represents the bandwidth



CHAPTER 6
SIMULATION

SIMULATION

6.1 PSCAD INTRODUCTION.

PSCAD (Power Systems Computer Aided Design) is a powerful and flexible graphical user interface to the world-renowned, EMTDC solution engine. PUCAO enables the user to schematically construct a circuit, run a simulation, analyse the results, and manage the data in a completely integrated graphical environment. Online plotting functions, controls and meters are also included, so that the user can alter system parameters during simulation run and view the results directly.

PSCAD comes complete with a library of pre-programmed and tested models, ranging from simple passive elements and control functions to more complex models, such as electric machines, FACTS devices, transmission lines and cables. If a particular model does not exist, PSCAD provides the flexibility of building custom models, either by assembling those graphically using existing models, or by utilizing an intuitively designed Design Editor PSCAD,

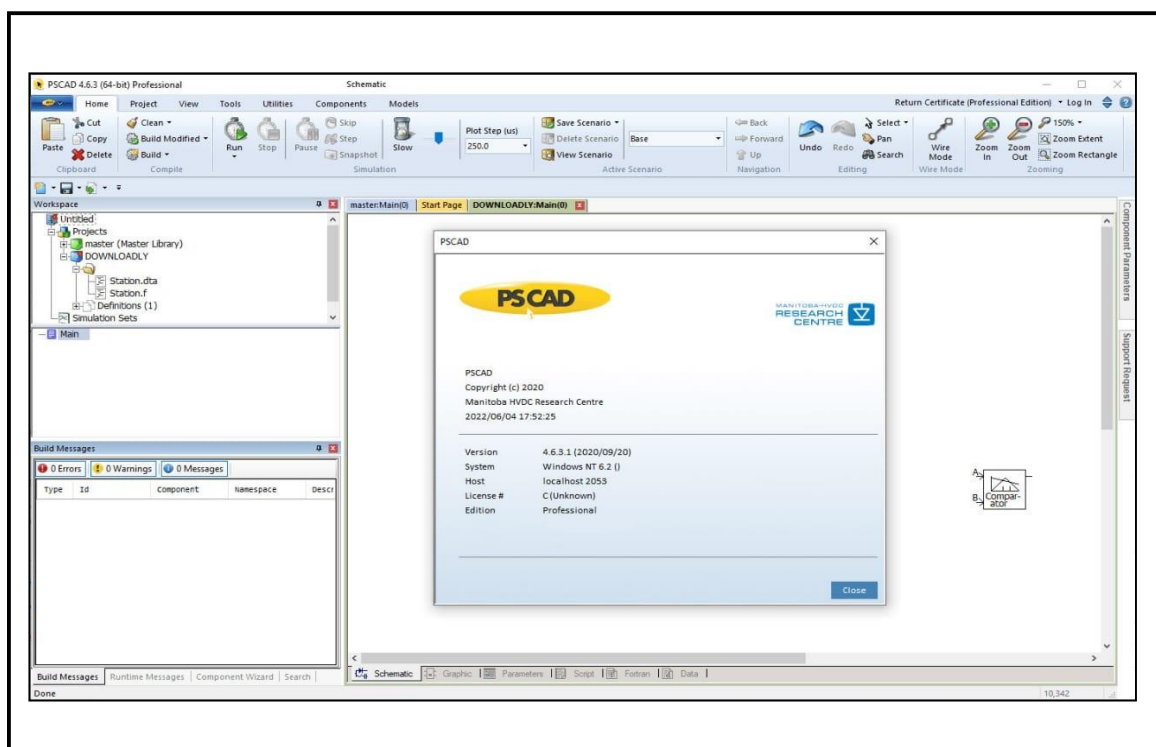


Fig 6.1 PSCAD Screen.

6.1.1 PSCAD Applications

PSCAD is used by engineers, researchers, and students from utilities, manufacturers, consultants, research, and academic institutes, it is used in planning, designing developing new concepts, testing ideas understanding what happened when equipment faced, commissioning and preparation of specification and tender documents, teaching and research.

The following are some of the studies that can be conducted with PSCAD:

- 1) Insulation coordination of AC and DC equipment.
- 2) Designing power electronic systems and controls including FACTS devices, filters, LOW voltage series and shunt compensation devices.
- 3) Incorporate the capabilities of MATLAB/Simulink directly into PSCAD/EMTDC.
- 4) Effects of DC currents and geomagnetically induced currents on power systems, inrush effects and ferro resonance.
- 5) Power quality analysis and improvement, including harmonic Impedance scans, motor starting sags and swells, non-linear loads. such as arc furnaces and associated flicker measurement.
- 6) Design of modern transportation systems (ships, rail, automotive) using power electronics.

6.2 SYSTEM UNDER STUDY.

Two Bus Test system is modelled in PSCAD environment. System Parameters mentioned in Appendix. Various types of faults (like LG, LL, LLG, LLL, LLLG) are Created at the middle of transmission line. A fault resistance considered is 0.01 Ω . The fault inception angles are varied from 0° to 360° in steps of 30° for each type of fault. Therefore, the total number of fault cases in this system is 65

Single Line Diagram

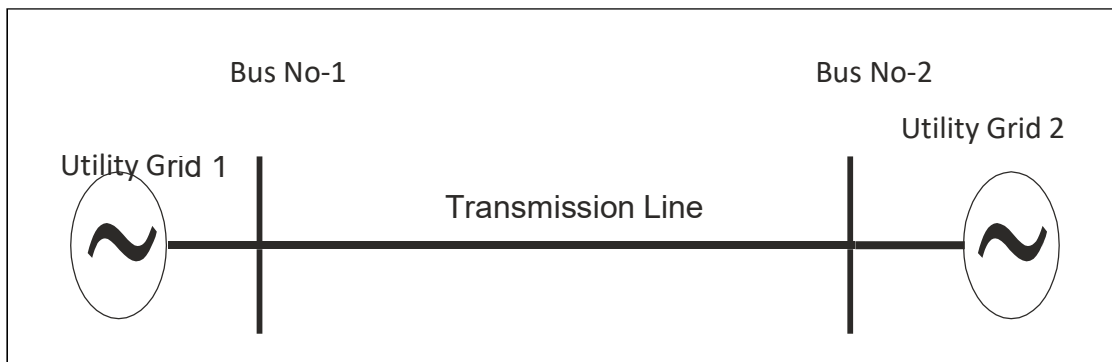


Fig 6.2 Single Line Diagram of Two Bus system [11]

6.3 SIMULATION IN PSCAD

- Duration of Run = 0.5 sec
- Solution Time Step = 0.00001 sec.
- Channel Plot Step = 0.00025 sec
- Sampling Frequency = 4000Hz (4kHz)
- Time to apply fault = 0.249 sec (at 0° FIA) During of fault = 0.166 sec

Simulation of Two Bus test system in PSCAD: Base Case.

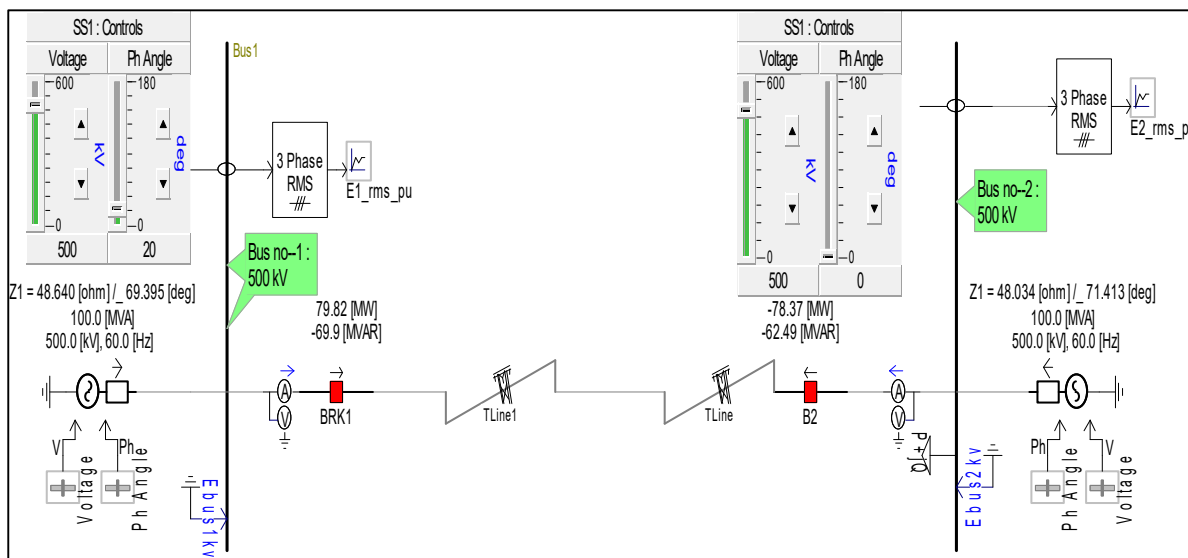


Fig 6.3 Two Bus system (without fault)

Simulation of Two Bus Test System During Various Types of Faults Like LG, LL, LLL, LLLG, LLLG) at the Middle of TL (FIA:0° to 360° in Steps of 30°)

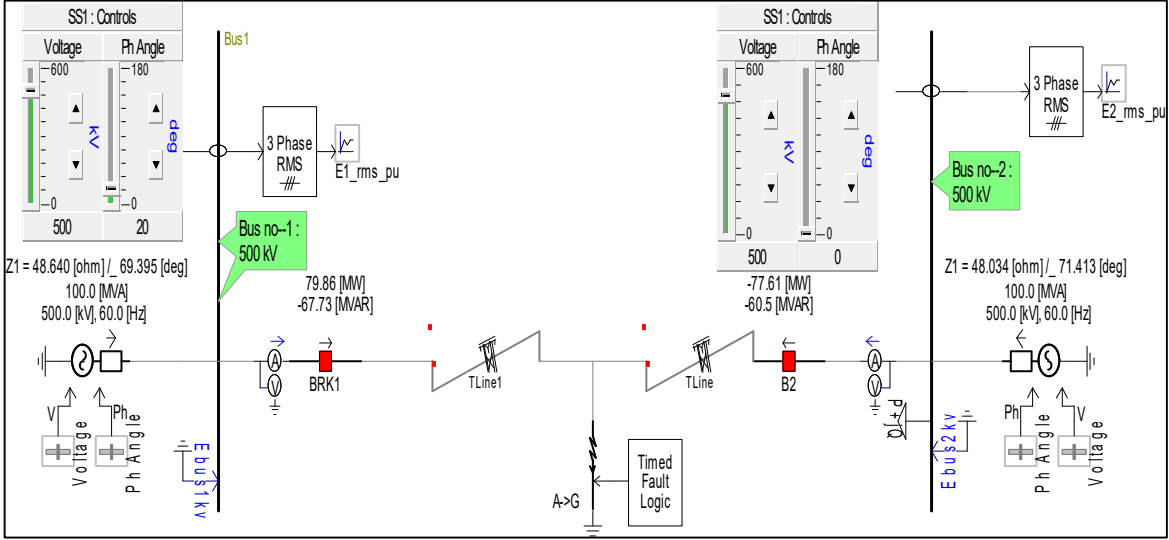


Fig 6.4 Two Bus system (with fault)

6.4 RESULT ANALYSIS IN PSCAD.

The analysis of Two Bus System during Various types of Faults likes (LG, LL, LLL, LLLG) at Middle of transmission line.

Base case with load

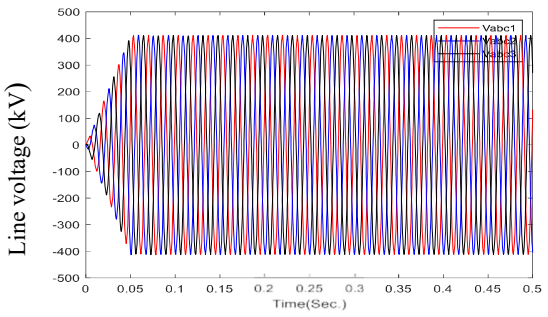


Fig 6.5 Line Voltage(kV) Vs Time Waveform (sec)

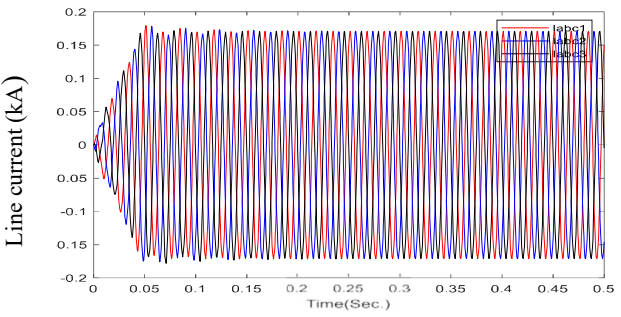


Fig 6.6 Line Current (kA) Vs Time Waveform (kA)

Current waveform of Two Bus Test System during Various types Fault likes (LG, LL, LLG, LLL, LLLG) at Middle of transmission line. (FIA:0°)

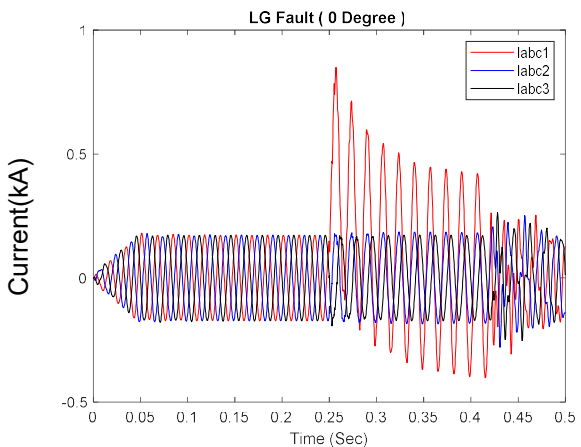


Fig 6.7 Line Current Vs TimeWaveform during LG Fault on T.L.

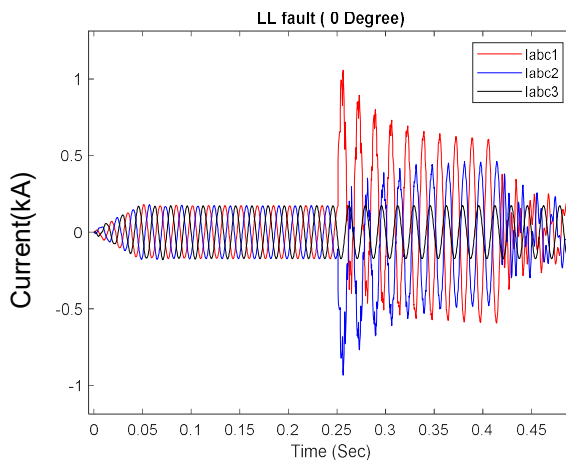


Fig 6.8 Line Current Vs Time Waveform during LL Fault on T.L

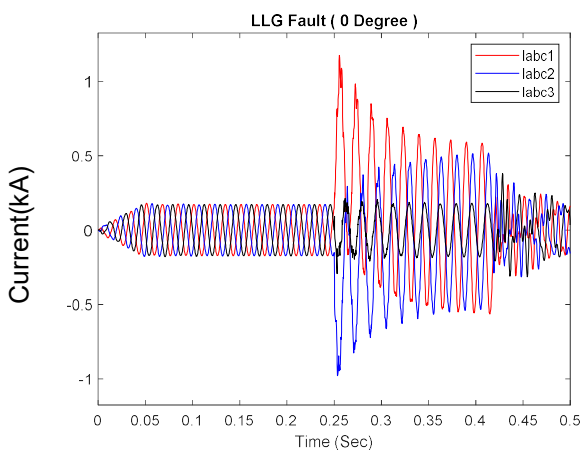


Fig 6.9 Line Current Vs TimeWaveform during LLG Fault on T.L

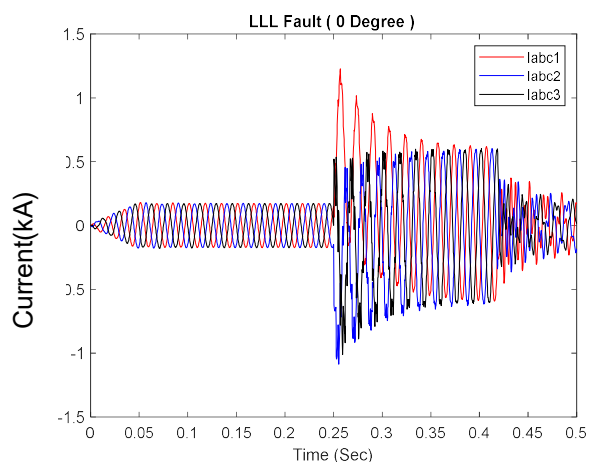


Fig 6.10 Line Current Vs TimeWaveform during LLL Fault on T.L

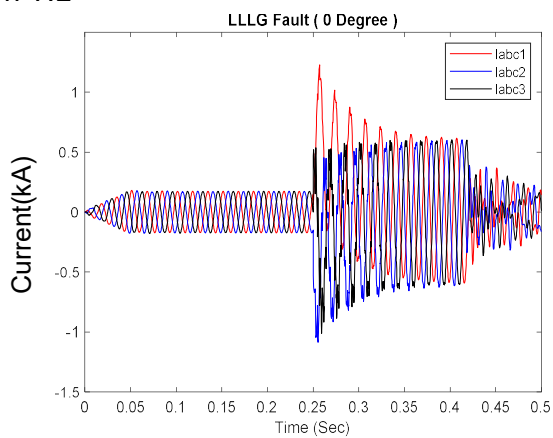


Fig 6.11 Line Current Vs TimeWaveform during LLLG Fault on T.L

CHAPTER 7
PROPOSED
METHODOLOGY

PROPOSED METHODOLOGY

In this project work detection and classification of overhead transmission line fault is carried out by using the following steps.

1. Simulation of Two Bus Test systems in PSCAD software.
2. Various types of faults (like LG, LL, LLG, LLL, and LLLG) are created at the middle transmission line at different fault inception angles (0° to 360° in steps of 30°)
3. Capturing of line current signals obtained at bus which is 110 km distance apart from the fault location with a duration of run 0.5sec and 4 kHz sampling frequency.
4. Output data of the Simulation is imported in MATLAB to apply S-Transform.
5. Formation of S-Matrix using S-Transform algorithm.
6. Extraction of feature median for fault detection.
7. Calculation of energy from the S-Matrix of current signals for input of the ANN model.
8. Formation of fault classification ANN model with neuron input-Hidden layer-Output layer configuration of 3-10-5.
9. Plotting, training, testing validation, and overall confusion matrixes for evaluation.

7.1 WORKFLOW OF SYSTEM

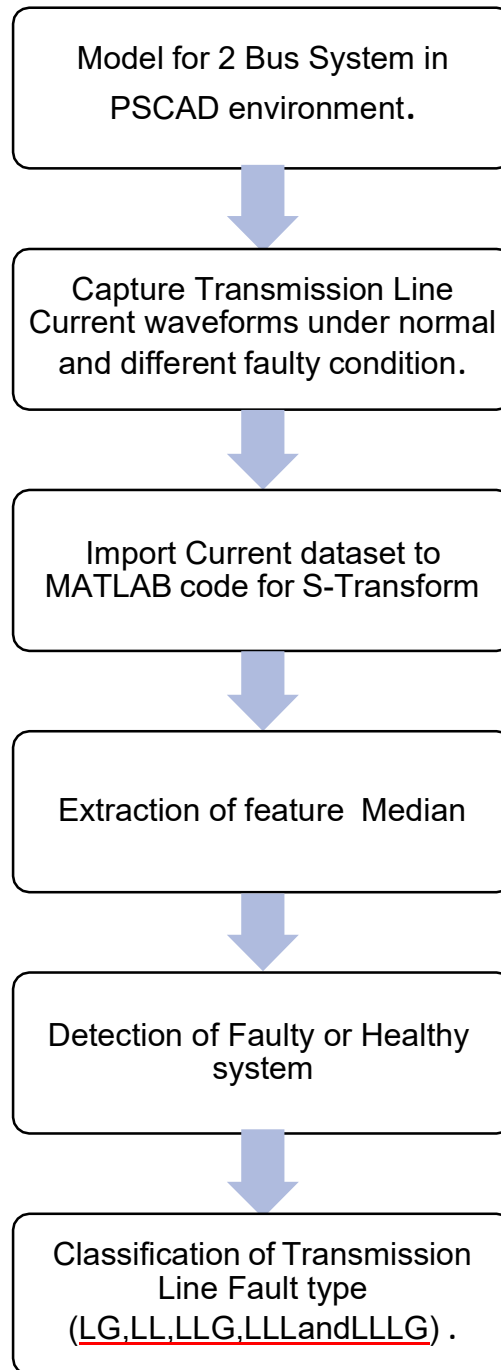
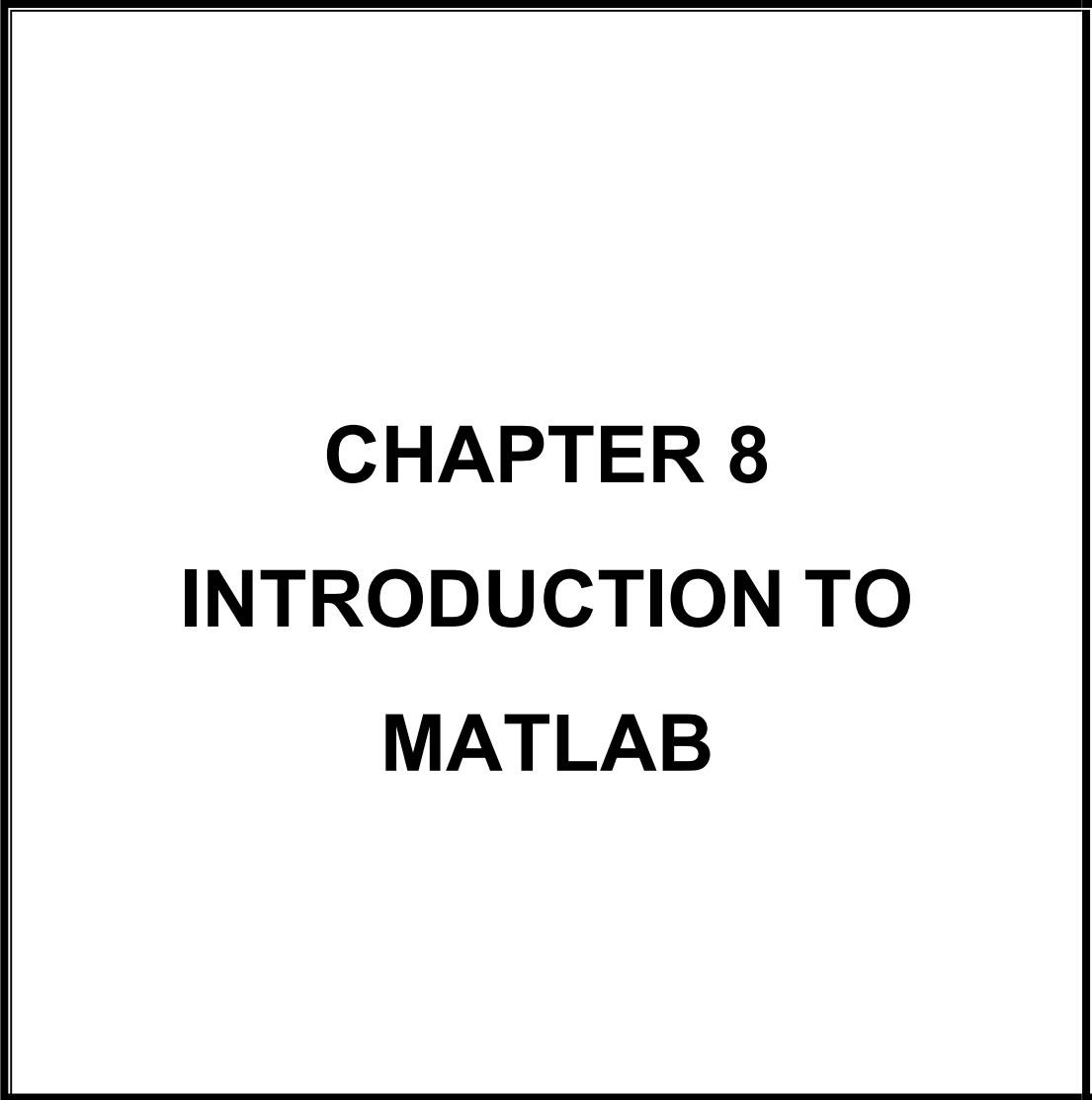


Fig.7.1 Project workflow



CHAPTER 8
INTRODUCTION TO
MATLAB

INTRODUCTION TO MATLAB

MATLAB is a high-performance language for technical computing. It integrates computation, visualization, and programming in an easy-to-use environment where problems and solutions are expressed in familiar mathematical notation.

Typical uses include:

- i. Math and computation
- ii. Algorithm development
- iii. Modelling, simulation, and prototyping
- iv. Data analysis, exploration, and visualization
- v. Scientific and engineering graphics

MATLAB is an interactive system whose basic data element is an array that does not require dimensioning. This allows you to solve many technical computing problems, especially those with matrix and vector formulations, in a fraction of the time it would take to write a program in a scalar non interactive language such as C.

MATLAB features a family of application-specific solutions called toolboxes. Very important to most users of MATLAB, toolboxes allow you to learn and apply specialized technology. Toolboxes are comprehensive collections of MATLAB functions (M-files) that extend the MATLAB environment to solve particular classes of problems. Areas in which toolboxes are available include signal processing, control system, neural network. Fuzzy logic, wavelets, simulation, and many others.

8.1 MATLAB APPLICATION

Some common applications of MATLAB in power systems

1) Power Flow Analysis: MATLAB can be used to perform power flow analysis, which calculates the steady-state voltages, currents, and power flows in a power system. MATLAB's optimization and numerical solver functions can be utilized to solve complex power flow equations.

- 2) **Fault Analysis and Protection:** MATLAB can be used for fault analysis in power systems, including fault location, fault type identification, and fault current calculations. It can also be used to design and evaluate protection schemes, such as relays and circuit breakers, for timely fault detection and isolation.
- 3) **Renewable Energy Integration:** MATLAB provides tools for modeling and simulating renewable energy systems, such as solar photovoltaic (PV) arrays, wind turbines, and energy storage systems. It enables analysis of their impact on power system stability, optimization of their integration, and evaluation of their performance under different scenarios.
- 4) **Dynamic System Simulation:** MATLAB's Simulink environment is widely used for dynamic system simulation in power systems. It allows the modelling and simulation of power system components like generators, transformers, and loads. This enables analysis of system behaviour under transient conditions, such as faults, load changes, and switching events.
- 5) **Optimization and Control:** MATLAB offers optimization algorithms that can be applied to power system problems, such as optimal power dispatch, economic load scheduling, and unit commitment. It can also be used for designing and implementing advanced control strategies, such as adaptive control, to improve system stability and efficiency.

CHAPTER 9

STOCKWELL TRANSFORM

STOCKWELL TRANSFORM

9.1 INTRODUCTION

Traditionally, the Fourier transform has been extensively used for analyzing the frequency contents of the signals. Besides, the FT is not an efficient analyzing tool for extracting the transient information of the non-stationary signals. Although the STFT divides the full-time interval into several small/equal-time intervals, can partly alleviate the problem, the STFT still has the limitation of a fixed window width. It is difficult to detect the occurrence times for very short duration and high-frequency signals. In order to avoid the disadvantages of both FT and STFT, the Wavelet Transform has been widely used for analysing the power quality problems.

The WT approach prepares a window that automatically adjusts to give proper resolutions of both the time and the frequency. In the approach, a larger resolution of time is provided to high-frequency components of a signal, and a larger resolution of frequency to low-frequency components. These features make the WT well suited for the analysis of the power system transients caused by various disturbances.

A new tool for monitoring power quality problems is introduced by scientist Stockwell in 1996 i.e., S-Transform. This transformation has ability to analyze different power quality problems simultaneously in both time and frequency domains. The detection and extraction of disturbance features from various types of electric power quality disturbances is important as-

Feature extraction is the key for pattern recognition, so it is the most important component of designing the system.

9.2 NEED OF S-TRANSFORM APPROACH?

What distinguishes the S-transform from the many time-frequency representations available is that the S-transform uniquely combines progressive resolution with

absolutely referenced phase information. Daubechies has stated that progressive resolution gives a fundamentally sounder time-frequency representation [10]. Absolutely referenced phase means that the phase information given by the S-transform is always referenced to time $t = 0$, which is also true for the phase given by the Fourier transform. This is true for each S-transform sample of the time-frequency space. This is in contrast to a wavelet approach, where the phase of the wavelet transform is relative to the centre (in time) of the analyzing wavelet. Thus, as the wavelet translates, the reference point of the phase translates. This is called “locally referenced phase” to distinguish it from the phase properties of the S-transform. From one point of view, local spectral analysis is a generalization of the global Fourier spectrum. In fact, since no record of observations is infinite, all discrete spectral analysis ever performed on measured data have been local (i.e., restricted to the time of observation). Thus, there must be a direct relationship between a local spectral representation and the global Fourier spectrum. This philosophy can be stated as the fundamental principle of S-transform analysis:

9.3 FAULT INDEX

A fault index is proposed to discriminate the faulty phases from the healthy phases. This fault index is also used to differentiate various types of faults on EHV transmission line.

Fault index is calculated using the following steps:

- (i) Current of all the phases is captured at bus 800 of the test system.
- (ii) Current signals are decomposed with the help of Stockwell Transform using a sampling frequency of 4kHz. The output of the Stockwell transform is obtained in the form of a matrix known as S-matrix.
- (iii) Median of S-matrix is obtained
- (iv) The absolute value of median is calculated, and it is designated as fault index.
- (v) This fault index is used to detect and locate the faults.

9.4 FEATURE EXTRACTION BY S-TRANSFORM

S-Transform is an improved version of continuous Wavelet Transform. The CWT, $W(\square, d)$ of a function $h(t)$ is defined as

$$W(r, d) = \int_{-\infty}^{\infty} h(t)w(t - r, d)dt \quad (11.4.1)$$

where, $W(r, d)$ is a scaled replica of the fundamental mother wavelet.

In equation (1) dilation factor d is inverse of frequency f . The dilation determines the width of the wavelet, and this controls the resolution. The S- Transform is obtained by multiplying the CWT with a phase factor, as defined below.

$$S(r, f) = e^{i2\pi fc}W(d, r) \quad (11.4.2)$$

where the mother wavelet for this particular case is defined as

$$w(t, f) = \frac{|f|}{\sqrt{2\pi}} e^{-\left(\frac{t^2 f^2}{2}\right)} e^{-j2\pi ft} \quad (11.4.3)$$

Thus, final form of the continuous S-transform is obtained as

$$S(r, f) = \int_{-\infty}^{\infty} h(t) \frac{|f|}{\sqrt{2\pi}} e^{-\frac{(r-t)^2 f^2}{2}} e^{-j2\pi ft} dt \quad (11.4.4)$$

and width of the Gaussian window is.

$$\sigma(f) = T = 1/|f| \quad (11.4.5)$$

9.5 PROPOSED FLOWCHART OF STOCKWELL TRANSFORM

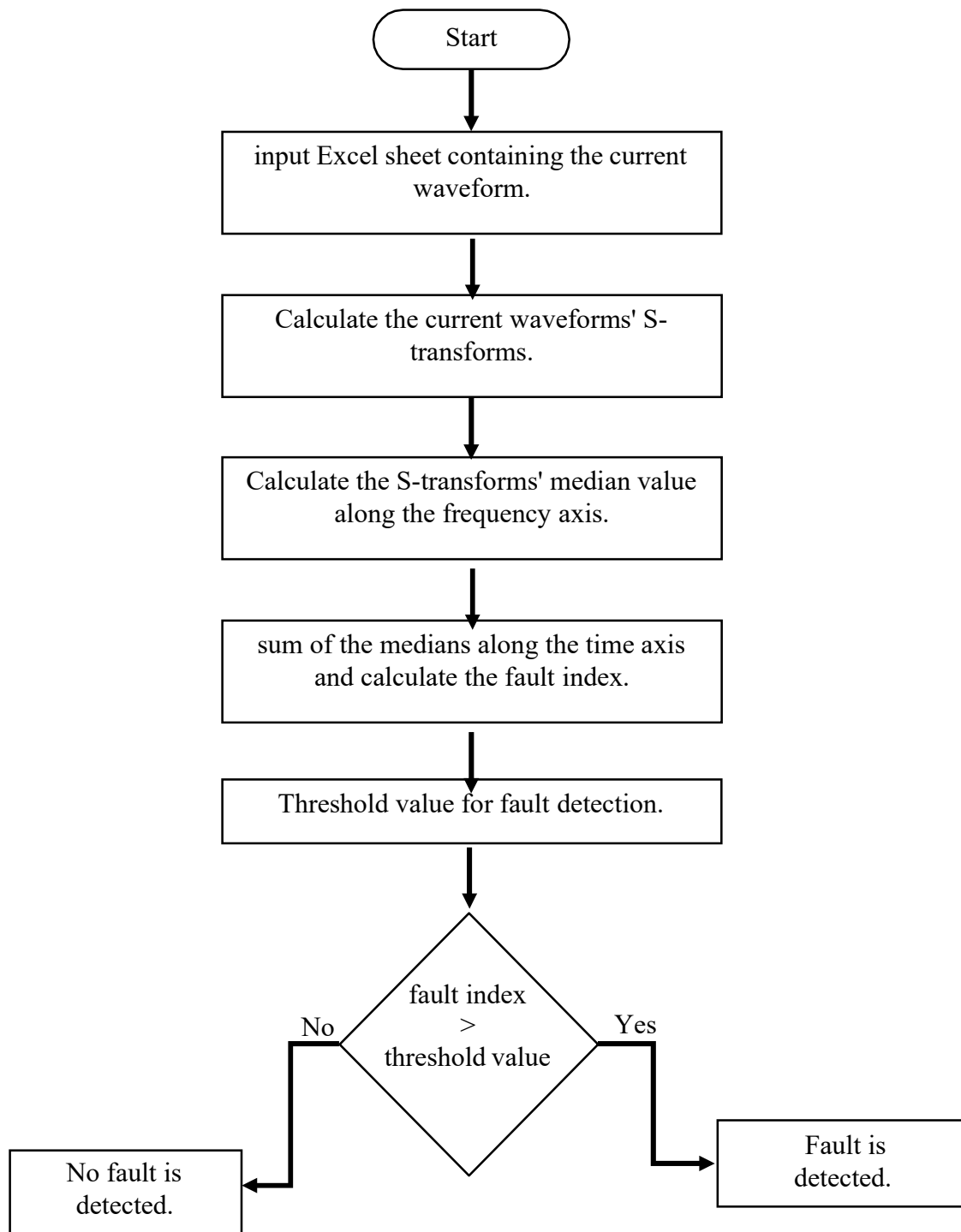


Fig.9.1 Flowchart of Stockwell Transform

CHAPTER 10

S-TRANSFORM RESULTS

AND DISCUSSION

S-TRANSFORM RESULTS AND DISCUSSION

The simulation results pertaining to the detection of faults in the power system lines using proposed fault index are elaborated in this section. Various types of faults (like LG, LL, LLG, LLL, LLLG) are created on Two Bus test network and line current captured at middle of the transmission line. The threshold value of fault is set at 0.85 after study of the 65 data sets of each fault with varying inception angle of 30-degree interval. Following subsections details the simulation results of various types of faults at 0° FIA.

10.1 PHASE TO GROUND (LG) FAULT

The fault involving one phase and ground (LG) has been simulated by grounding the phase-A. Waveforms of current in all phases during the event of LG fault created on phase-A are shown in Fig.10.1. This is observed that current magnitude of phase-A increases from the value of 172 A to 800 A. However, the magnitude of current in all the healthy phases (phase-A & B) remains the same.

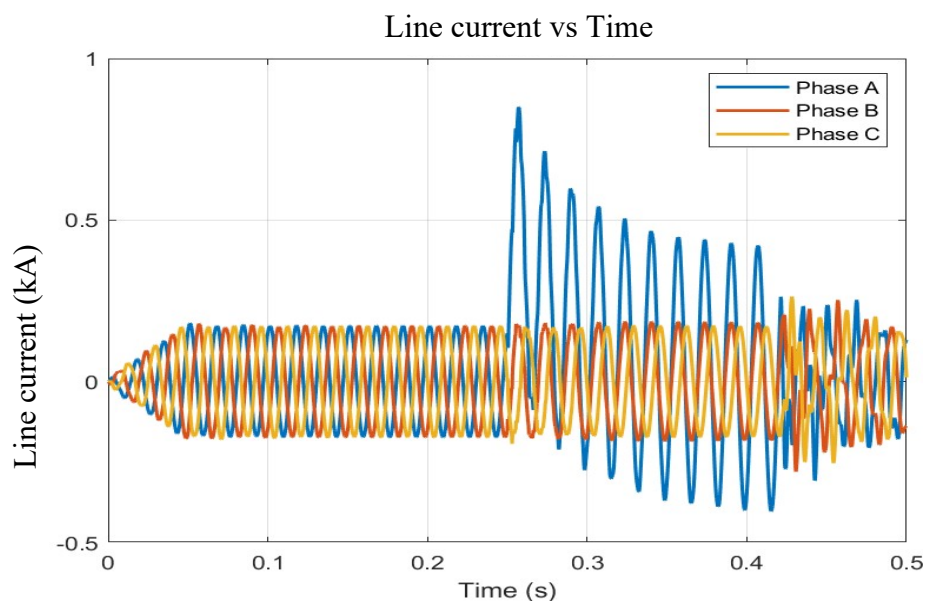


Fig.10.1 Line Current Vs Time During LG Fault on T.L

The values of proposed fault index for all the three phases in the event of LG fault simulated on phase-A have been shown in Fig. 10.2 This is observed and identified that value of proposed fault index is higher than the threshold value (0.085 in this case) whereas the fault indices have values lower than the threshold for the

healthy phases. The fault index value for the faulty phase is 0.863. Hence, the LG fault is detected effectively.

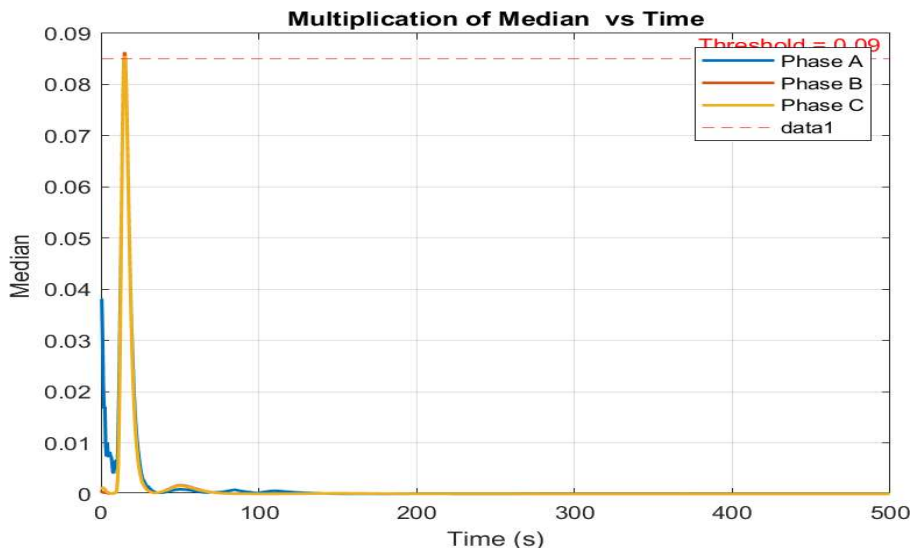


Fig.10.2 Fault index calculated using current waveform during LG fault.

10.2 DOUBLE LINE (LL) FAULT

The fault involving two phases without the involvement of ground (LL) is simulated by short circuiting the phases A and B. Three-phase current waveforms in the event of LL fault on phases A & B are illustrated in Fig.10.3. This is observed and identified that current magnitude of phases A & B has increased from 172 A to 1000 A. However, the magnitude of current in the phase-C (healthy phase) remains same as before the fault occurrence.

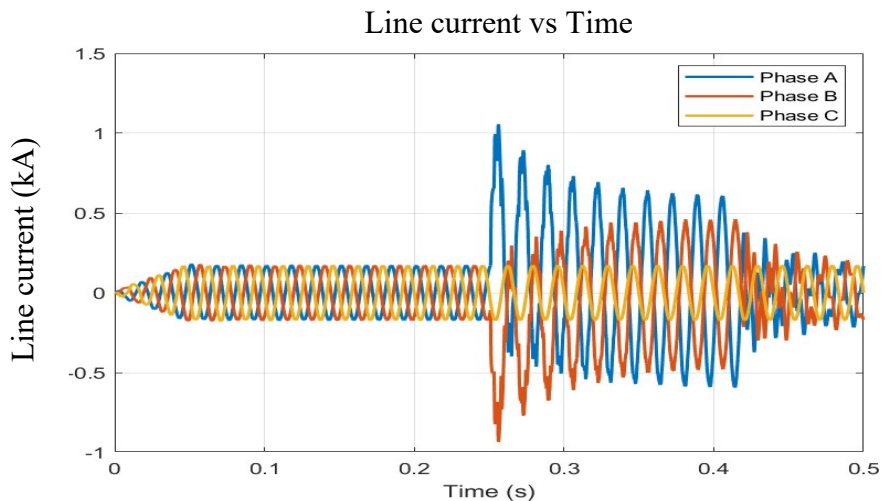


Fig.10.3 Line Current Vs Time During LL Fault on T.L

The values of proposed fault indices for all the three phases in the event of LL fault involving the phases A&B have been illustrated in Fig.10.4 This is observed and identified that fault indices pertaining to the faulty phases A & B is higher relative to threshold value and equal to 0.0864363. The fault index for the healthy phase (phase C) is below the threshold value and equal to 0.085. Hence, the LL fault is effectively detected using the proposed algorithm.

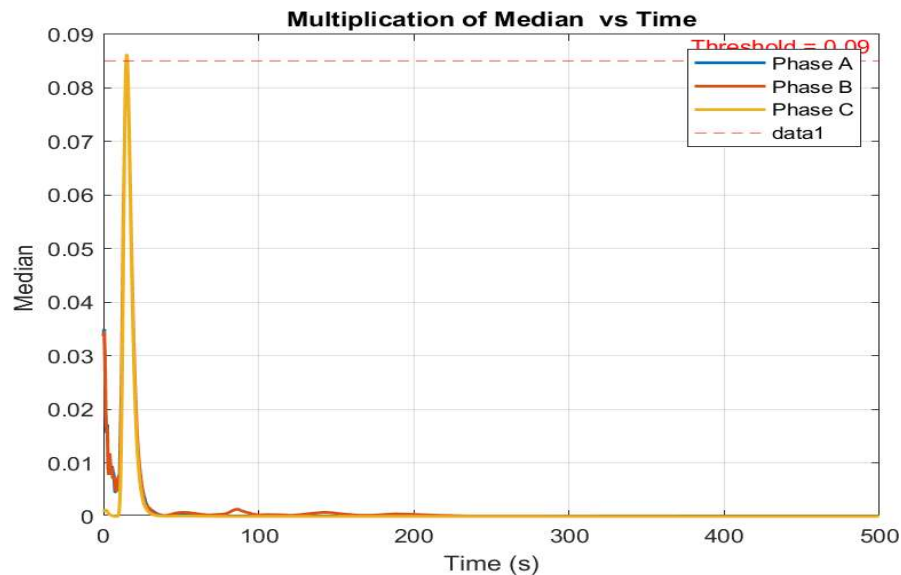


Fig.10.4. Fault index calculated using current waveform during LL fault.

10.3. DOUBLE LINE TO GROUND (LLG) FAULT

The fault involving two phases and ground (LLG) has been simulated by simultaneously grounding the phases A and B. The current waveforms related to all the three-phase in the event of occurrence of LLG fault are shown in Fig.10.5. This is observed that magnitude of current in phases A & B has been increased from 172 A to 1200 A. However, the magnitude of current in phase-C (healthy phase) remains the same as before the fault occurrence.

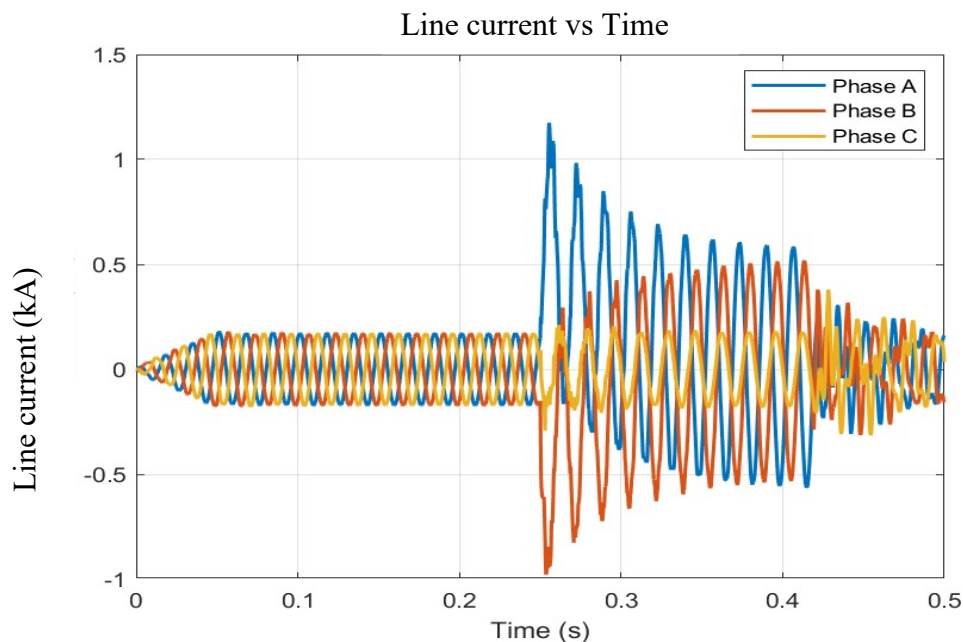


Fig 10.5. Line Current Vs Time During LLG Fault on T.L

The values of proposed fault index for all the three phases in the event of LLG fault with the involvement of phases A&B have been shown in Fig.10.6. This is identified and observed that values of fault indices pertaining to faulty phases A & B are higher compared to threshold value and equal to 0.085. The fault index for the healthy phase (phase C) is below the threshold value and equal to 0.0865383. the LLG fault is effectively detected using the proposed algorithm.

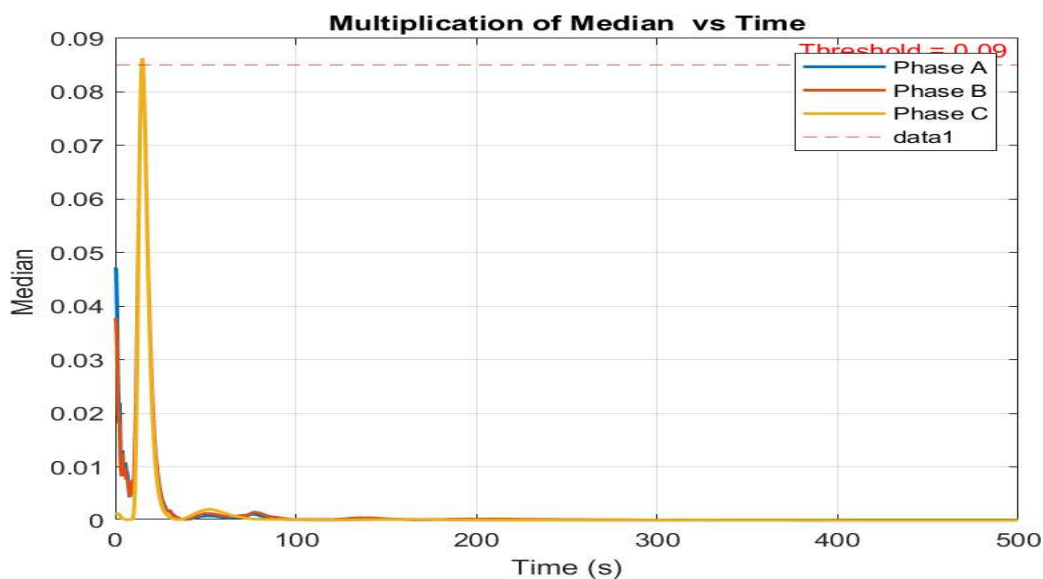


Fig.10.6. Fault index calculated using current waveform during LLG fault

10.4. THREE PHASE LINE (LLL)FAULT

All the three phases are simultaneously simulated without the ground (LLL). Three phase current waveforms during fault period are illustrated in Fig.10.7. This is observed and predicted that current magnitude of all three phases has been increased from 172 A to 1300 A.

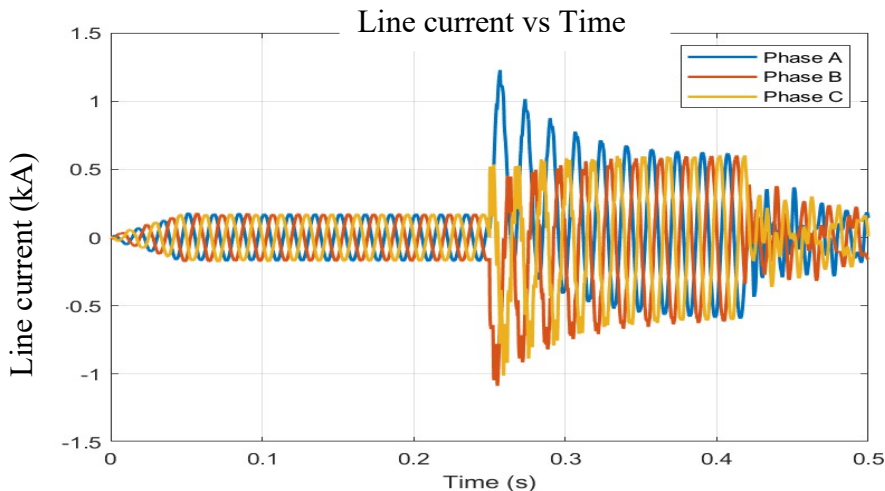


Fig.10.7 Line Current Vs Time During LLL Fault on T.L

The values of proposed fault index for all the three phases during the LLL fault have been shown in Fig.10.8. This is observed predicted that values of fault indices of all phases are higher compared to the threshold value and above 0.085. The fault index is below the threshold value and equal to 0.0866383 Hence, the LLL fault is effectively detected using the proposed algorithm.

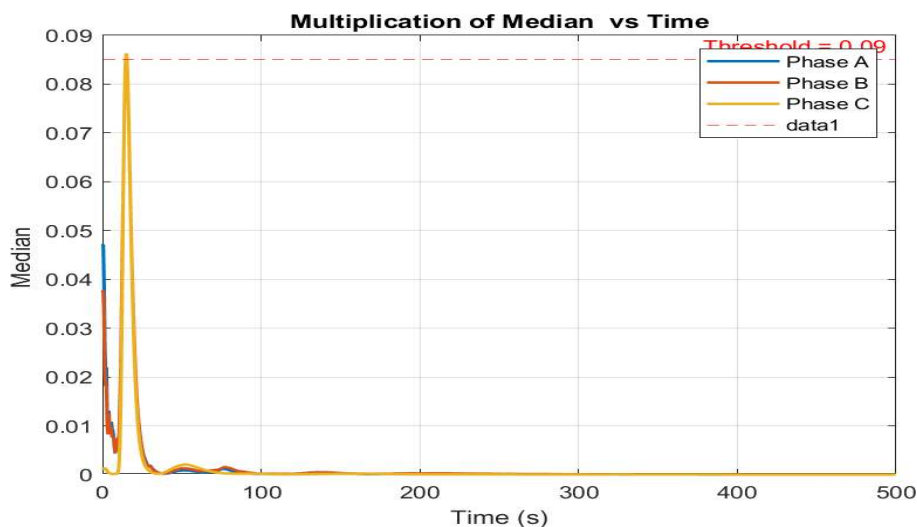


Fig. 10.8 Fault index calculated using current waveform during LG fault.

10.5 Three Phase Fault Involving (LLLG) Ground

All the three phases are simultaneously grounded to simulate the three phase to ground fault (LLLG). Three phase current waveforms during fault period are illustrated in Fig. 8.9 This is observed and predicted that current magnitude of all three phases has been increased from 172 A to 1350 A. However, the magnitude of current in phase-C (healthy phase) remains the same as before the fault occurrence.

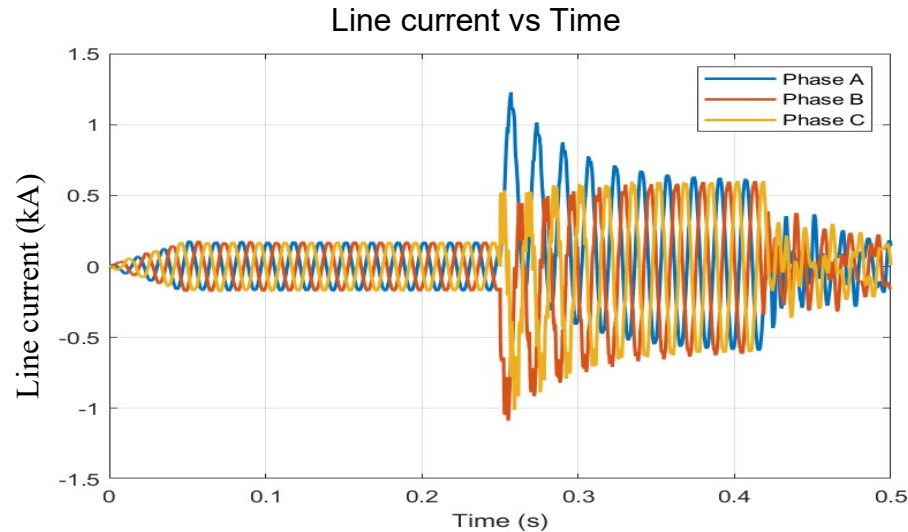


Fig.10.9 Line Current Vs Time During LLLG Fault on T.L

The values of proposed fault index for all the three phases during the LLLG fault have been shown in Fig 10.10. This is observed predicted that values of fault indices of all phases are higher compared to the threshold value and above 0.085. The fault index is below the threshold value and equal to 0.0867255 Hence, the LLLG fault is effectively detected using the proposed algorithm.

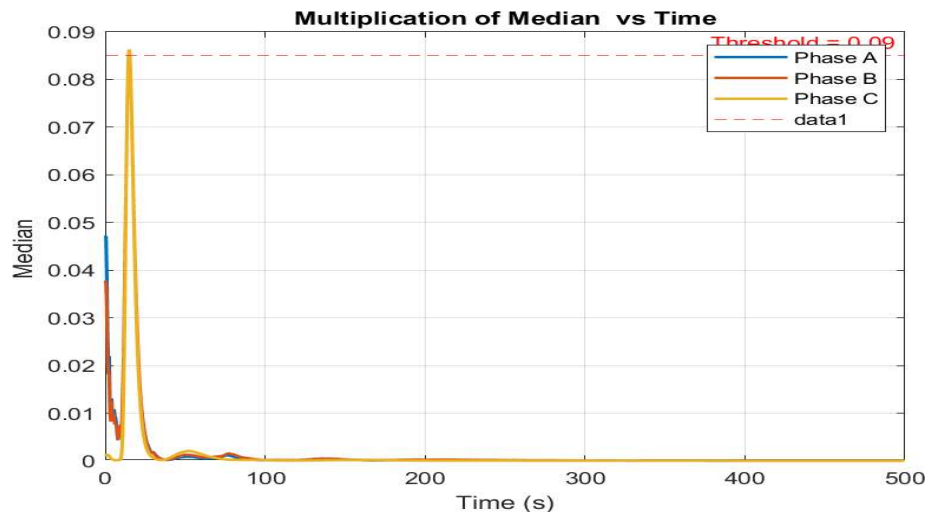


Fig.10.10. Fault index calculated using current waveform during LG fault.

10.6 FAULT INDEX MAGNITUDE AT DIFFERENT FAULT.

Fault Type	Fault Index Magnitude
LG	0.0863458
LL	0.0864363
LLG	0.0865383
LLL	0.0866383
LLLG	0.0867255

Table 10.1 Types of Faults and Magnitude

CHAPTER 11
ARTIFICIAL NEURAL
NETWORKS

ARTIFICIAL NEURAL NETWORKS

11.1 Introduction

ANN is defined as a computing system made up of a number of simple, highly interconnected processing elements, which process information by their dynamic state response to external inputs. An artificial neural network is a system based on the operation of biological neural networks, in other words, is an emulation of biological neural system. Why would be necessary the implementation of artificial neural networks? Although computing these days is truly advanced, there are certain tasks that a program made for a common microprocessor is unable to perform; even so a software implementation of a neural network can be made with their advantages and disadvantages.

11.2 Architecture of ANN:

Neural networks are typically organized in layers. Layers are made of several interconnected 'nodes' which contain 'activation function'. Patterns are presented to the network via the 'input layer', which communicates to or more 'hidden layers' where the actual processing is done via a system of weighted 'connection'. The hidden layers then link to an 'output layer' where the answer is output as shown in the graphic below.

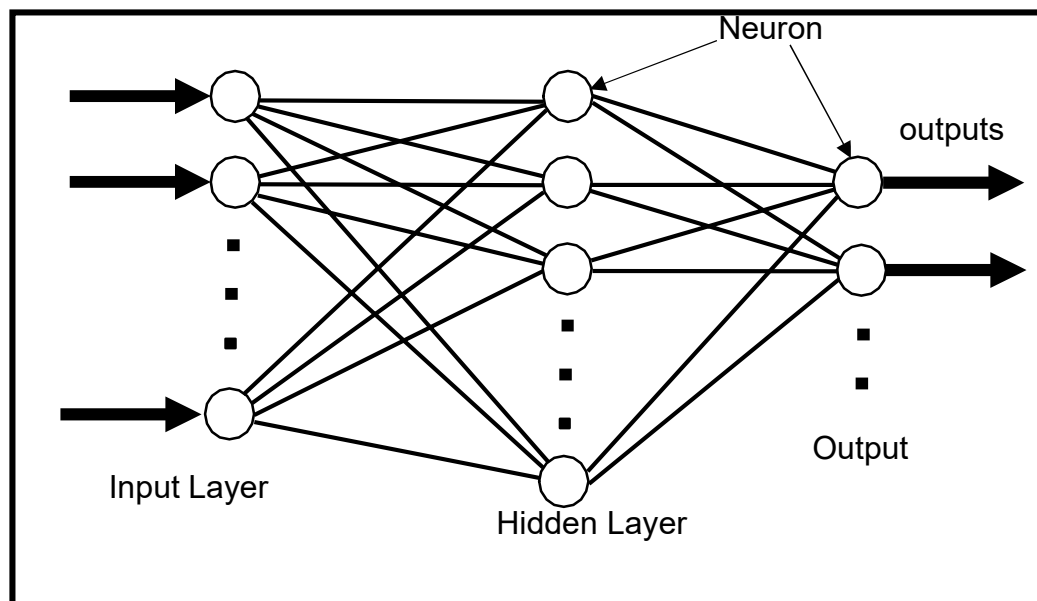


Fig.11.1 ANN architecture

An input is presented to the neural network and a corresponding desired or a target response set at the output (when this is the case the training is called supervised). An error is composed from the difference between the desired response and the system output. This error information is fed back to the system and adjusts the system parameters in a systematic fashion (the learning rule). The process is repeated until the performance is acceptable. It is clear from this description that the performance hinges heavily on the data. If one does not have data that cover a significant portion of the operating conditions or if they are noisy, then neural network technology is probably not the right solution. On the other hand, if there is plenty of data and the problem is poorly understood to derive an approximate model, then neural network technology is a good choice. In artificial neural networks, the designer chooses the network topology, the performance function, the learning rule, and the criterion to stop the training phase, but the system automatically adjusts the parameters. So, it is difficult to bring a priority information into the design.

11.3 BACK PROPAGATION LEARNING.

The simple perceptron is just able to handle linearly separable or linearly independent problems. By taking the partial derivative of the error of the network with respect to each weight, we will learn a little about the direction the error of the network is moving. In fact, if we take the negative of this derivative (i.e., the rate change of the error as the value of the weight increases) and then proceed to add it to the weight, the error will decrease until it reaches local minima. This makes sense because if the derivative is Positive, this tells us that the error is increasing when the weight is increasing. The obvious thing to do then is to add a negative value to the weight and vice versa if the derivative is negative. Because the taking of these partial derivatives and then applying them to each of the weights takes Place, starting from the output layer to hidden layer weights, then the hidden layer to input layer weights (as it turns out, this is necessary since changing these set of weights requires that we know the Partial derivatives calculated in the layer downstream), this algorithm has been called the backpropagation algorithm A neural network can be trained in two different modes: online and batch modes. The

number of weight updates of the two methods for the same number of data presentations is very different. The online method weight updates are computed for each input data sample, and the weights are modified after each sample. An alternative solution is to compute the weight update for each input sample but store these values during one pass through the training set which is called an epoch. At the end of the epoch, all the contributions are added, and only then the weights will be updated with the composite value. This method adapts the weights with a cumulative weight update, so it will follow the gradient more closely.

It is called the batch-training mode. Training basically involves feeding training samples as input vectors through a neural network, calculating the error of the output layer, and then adjusting the weights of the network to minimize the error. The average of all the squared errors (E) for the outputs is computed to make the derivative easier. Once the error is computed, the weights can be updated one by one. In the batched mode variant, the descent is based on the gradient ∇E for the total training set.

The momentum term determines the effect of past weight changes on the current direction of movement in the weight space. A good choice of both η and α are required for the training success and the speed of the neural network learning. It has been proven that backpropagation learning with sufficient hidden layers can approximate any nonlinear function to arbitrary accuracy. This makes backpropagation learning neural network a good candidate for signal prediction and system modelling.

11.4 BACK PROPAGATION ALGORITHM.

The output values O_j of a given input pattern X_i do not always correspond to their predetermined value R_j . The error E_j is given by the difference of R_j and O_j and is to be minimized by the weight changes. The error of a neuron j in the output layer is:

$$E_j = \frac{1}{2} (R_j - O_j)^2 \quad (11.4.1)$$

The total error E of an output layer is.

$$E = \sum_j E_j = \frac{1}{2} \sum_j (R_j - O_j)^2 \quad (11.4.2)$$

So, need to minimize the error E , with respect to the weight changes (ΔW_{ij}).

follow the delta rule to incorporate the learning rate α , along with the gradient descent algorithm techniques to defame the weight change.

$$\Delta W_{kj} = -\alpha \cdot \frac{\partial E}{\partial W_{kj}}; 0 < \alpha \leq 1 \quad (11.4.3)$$

If the gradient $\frac{\partial E}{\partial W_{kj}}$ is positive, then the weight change should be negative and vice versa. Hence, a minus sign is added at the right-hand side of (.

Considering neuron.

$$\Delta W_{kj} = -\alpha \cdot \frac{\partial E}{\partial W_{kj}} \quad (11.4.4)$$

Using a sigmoid transfer function $T_j(S_j)$, the output O_j is defined as:

$$O_j = T_j(S_j) = \frac{1}{1 + e^{-S_j}} \quad (11.4.5)$$

For the hidden layer input) to the output layer,

$$S_j = \sum_k W_{kj} \cdot H_k \quad (11.4.6)$$

From (11.4.3) and (11.4.4),

$$\begin{aligned} \Delta W_{kj} &= -\alpha \cdot \frac{\partial E_j}{\partial W_{kj}} = -\alpha \cdot \frac{\partial E_j}{\partial O_j} \cdot \frac{\partial O_j}{\partial W_{kj}} \\ &= -\alpha \cdot \frac{\partial E_j}{\partial O_j} \cdot \frac{\partial O_j}{\partial S_j} \cdot \frac{\partial S_j}{\partial W_{kj}} \end{aligned} \quad (11.4.7)$$

From (11.4.1) we get,

$$\frac{\partial E_j}{\partial O_j} = \frac{-2}{2} (R_j - O_j) = (R_j - O_j) \quad (11.4.8)$$

Using (11.4.5) we get,

$$\frac{\partial O_j}{\partial S_j} = O_j (1 - O_j) \quad (11.4.9)$$

From (11.4.6) we get,

$$\frac{\partial S_j}{\partial W_{kj}} = \frac{\partial (\sum_k W_{kj} \cdot H_k)}{\partial W_{kj}} = H_k \quad (11.4.10)$$

Combining (11.4.7) to (11.4.10), we finally get,

$$\Delta W_{kj} = \alpha \cdot (R_j - O_j) \cdot O_j (1 - O_j) H_k \quad (11.4.11)$$

So, new weights are,

$$W'_{kj} = W_{kj} + \Delta W_{kj} \quad (11.4.12)$$

The error of the output layer is back propagated to the weights of the hidden and the input layer. ΔW_{kj} is the change in weights from the output layer to the hidden layer. The back propagated error E_k of the hidden layer is given by:

$$E_k = \sum E_j = \frac{1}{2} \sum_j (R_j - O_j)^2 \quad (11.4.13)$$

Corresponding to (11.4.2) is the weight change ΔW_{ik} . We introduce a new learning rate α . We finally get the weight changes in the hidden layer as:

$$\Delta W_{ik} = \alpha' \cdot \sum_j (R_j - O_j) \cdot O_j(1 - O_j) \cdot W_{kj} \cdot H_k(1 - H_k)X_i \quad (11.4.14)$$

It has been proven that back propagation learning with sufficient hidden layers can approximate any nonlinear function to arbitrary accuracy. This makes back propagation learning neural network a good candidate for signal prediction and system modeling.

11.5 ANN Design for Fault Classification

The network for fault classification has 3 inputs and 5 outputs where it was designed with 200 training data set for each input and output. The training data consists of 65 samples for nine faults and no fault as input data. The five target output data presented fault state of LG, LL, LLG, LLL, LLLG faults, where 1 and 0 are specified. The Scaled Conjugate Gradient training technique was adopted since it required less memory and was suitable in low memory situations. To classify the issue in the neural network, a pattern recognition tool was employed. The input to the ANN module is the energy of the three phases extracted from ST matrix by normalizing in the frequency domain. Training data is 75% while testing data is 25%.

CHAPTER 12
RESULT AND DISCUSSION

RESULT AND DISCUSSION:

S-Matrix is obtained at the output of S transform program. It is complex matrix contain real and imaginary values. Normalized frequency is used to calculate energy of the signal. Energy of the voltage and current signals are calculated for different faults at different fault inception angles from 0 to 360°.

Signal energy is calculated based on Parseval's Theorem. This theorem states that the energy of a signal remains the same whether it is computed in a signal domain (time) or in a transform domain (frequency). If a,b,c are the three phases ia,ib,ic are the current signals corresponding to a,b,c phases. Then their energies are denoted by Ela,EIb,EIc for currents.

Fault Inception Angle	EIa	EIb	EIc
0°	18.15301	18.15301	18.15301
30°	18.15301	18.15301	18.15301
60°	18.15301	18.15301	18.15301
90°	18.15301	18.15301	18.15301
120°	18.15301	18.15301	18.15301
150°	18.15301	18.15301	18.15301
180°	9.151757	17.22928	18.15301
210°	8.863444	16.89933	17.82104
240°	8.741444	16.58853	17.51963
270°	8.670629	16.46629	17.40093
300°	8.743039	16.61092	17.56075
330°	8.923786	16.97451	17.95929
360°	9.075806	17.30019	18.3026

Table:12.1 Energy values of current signals during LG fault

Fault Inception Angle	E_{la}	E_{lb}	E_{lc}
0°	7.851549	7.851549	16.51662
30°	7.851549	9.115056	16.51662
60°	8.122008	9.625549	16.51662
90°	8.241309	9.884804	16.51662
120°	8.397613	9.994517	16.51662
150°	8.138753	9.576206	16.51662
180°	7.798884	8.998516	16.51635
210°	7.602506	8.057117	19.92216
240°	7.581488	8.621089	16.51662
270°	7.760469	8.948831	16.51662
300°	8.01791	9.432898	16.51662
330°	8.214481	9.824392	16.51662
360°	8.178633	9.814481	16.51662

Table:12.2 Energy values of current signals during LL faults

Fault Inception Angle	E_{la}	E_{lb}	E_{lc}
0°	7.676609	8.093646	19.83285
30°	7.96462	8.333887	7.96462
60°	8.226078	8.667999	19.27287
90°	8.235578	8.891331	18.98339
120°	8.348486	8.98218	17.98487
150°	7.719699	8.496304	19.76388
180°	7.719699	8.496304	19.76388
210°	8.416573	7.816279	8.583784
240°	7.602506	8.057117	19.92216
270°	7.912506	8.213754	19.63359
300°	8.148608	8.546721	19.42023
330°	8.292208	8.813182	18.99183
360°	8.424496	9.023536	17.96012

Table12.3: Energy values of current signals during LLG faults

Fault Inception Angle	E_{la}	E_{lb}	E_{lc}
0°	7.976667	8.248483	8.461028
30°	7.952094	8.583368	8.100084
60°	7.958975	8.622461	8.190547
90°	8.307414	8.408477	7.913931
120°	8.557546	8.501479	7.758848
150°	8.584213	8.117207	8.022045
180°	8.317277	7.905643	8.382735
210°	7.978283	7.811595	8.563224
240°	8.055293	8.114493	2.620241
270°	8.002929	8.480773	8.480773
300°	7.864769	8.622606	8.306648
330°	8.189737	8.509591	7.968585
360°	8.535436	8.159883	7.903682

Table12.4: Energy values of current signals during LLL faults

Fault Inception Angle	E_{la}	E_{lb}	E_{lc}
0°	7.768833	8.200753	8.51214
30°	7.754128	8.51869	8.159298
60°	7.983948	8.579871	7.741057
90°	7.983948	8.579871	7.741051
120°	8.551135	8.075135	7.761468
150°	8.550299	7.675911	8.030122
180°	8.381291	7.704264	8.339123
210°	7.590632	8.635679	16.51662
240°	7.609449	8.115094	8.502308
270°	7.767216	8.424845	8.291956
300°	7.867216	8.582027	7.872047
330°	8.135499	8.552919	7.756322
360°	8.465271	8.215488	7.708018

Table12.5: Energy values of current signals for LLLG faults

Table no.12.1,12.2,12.3,12.4,12.5 shows energy values of current signals for LG, LL, LLG,LLL,LLG faults on transmission line of two Bus test system. The energy values Extracted by normalising the ST matrix in frequency domain. All the faults have been created with a varied inception angle in three stages with the angle difference 30° from 0° to 360° .

In this configuration three neuron input, ten number of hidden layer and five number of output was Selected. It gives best performance for transmission line fault classification. There are four confusion matrix which is training, validation, testing and overall.

Output Class	LG fault	LL	LLG	LLL	LLL G	Percentage
LG fault	8 25.0%	0 0.0%	0 0.0%	0 0.0%	0 0.0%	100% 0.0%
LL	0 0.0%	6 18.8%	0 0.0%	0 0.0%	0 0.0%	100% 0.0%
LLG	0 0.0%	0 0.0%	7 21.9%	0 0.0%	0 0.0%	100% 0.0%
LLL	0 0.0%	0 0.0%	0 0.0%	5 15.6%	0 0.0%	100% 0.0%
LLL G	0 0.0%	0 0.0%	0 0.0%	0 0.0%	6 18.8%	100% 0.0%
Percentage	100% 0.0%	100% 0.0%	100% 0.0%	100% 0.0%	100% 0.0%	100% 0.0%
	LG fault	LL	LLG	LLL	LLL G	Percentage
	Target Class					

Fig.12.1. Training confusion matrix.

Figure 12.1. shows training confusion matrix with 100% efficiency of LG, LL, LLG, LLL, LLLG faults on transmission line with two bus test system under study.

Testing Confusion Matrix

Output Class	LG fault	5 15.2%	0 0.0%	0 0.0%	0 0.0%	0 0.0%	100% 0.0%
	LL	0 0.0%	8 24.2%	0 0.0%	0 0.0%	1 3.0%	88.9% 11.1%
	LLG	0 0.0%	1 3.0%	5 15.2%	0 0.0%	0 0.0%	83.3% 16.7%
	LLL	0 0.0%	0 0.0%	0 0.0%	6 18.2%	2 6.1%	75.0% 25.0%
	LLLG	0 0.0%	0 0.0%	0 0.0%	1 3.0%	4 12.1%	80.0% 20.0%
	Percentage	100% 0.0%	88.9% 11.1%	100% 0.0%	85.7% 14.3%	57.1% 42.9%	84.8% 15.2%
		LG fault	LL	LLG	LLL	LLLG	Percentage
		Target Class					

Fig 12.2. Testing confusion matrix.

Figure 12.2. shows the testing confusion matrix with 84.8% as overall efficiency. LG, LL, LLG, LLL, LLLG faults have been tested with an efficiency of 88.9%, 83.3%, 75.0%, 80% respectively.

Validation Confusion Matrix

Output Class	LG fault	5 22.7%	0 0.0%	0 0.0%	0 0.0%	0 0.0%	100% 0.0%
	LL	0 0.0%	4 18.2%	0 0.0%	0 0.0%	0 0.0%	100% 0.0%
	LLG	0 0.0%	1 4.5%	3 13.6%	0 0.0%	0 0.0%	75.0% 25.0%
	LLL	0 0.0%	0 0.0%	1 4.5%	7 31.8%	1 4.5%	77.8% 22.2%
	LLLG	0 0.0%	0 0.0%	0 0.0%	0 0.0%	0 0.0%	NaN% NaN%
	Percentage	100% 0.0%	80.0% 20.0%	75.0% 25.0%	100% 0.0%	0.0% 100%	86.4% 13.6%
		LG fault	LL	LLG	LLL	LLLG	Percentage
		Target Class					

Fig.12.3. Validation confusion matrix.

Figure 12.3. shows the testing confusion matrix with 86.4% as overall efficiency. LG, LL, LLG, LLL, LLLG faults have been tested with an efficiency of 88.9%, 83.3%, 75.0%, 80% respectively.

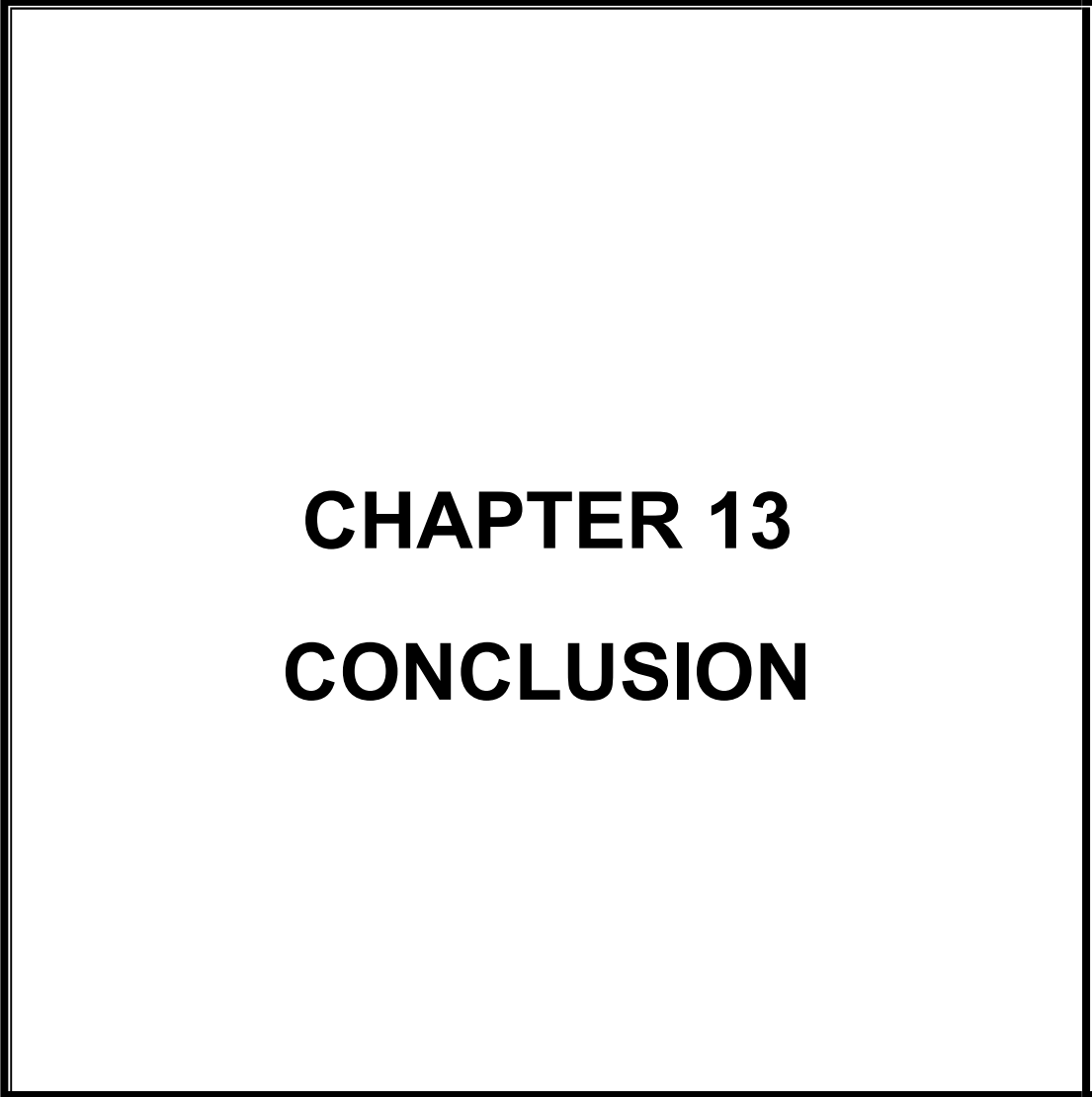
Overall Confusion Matrix

Output Class	LG fault	13 20.0%	0 0.0%	0 0.0%	0 0.0%	0 0.0%	100% 0.0%
	LL	0 0.0%	12 18.5%	0 0.0%	0 0.0%	0 0.0%	100% 0.0%
	LLG	0 0.0%	1 1.5%	13 20.0%	0 0.0%	1 1.5%	86.7% 13.3%
	LLL	0 0.0%	0 0.0%	0 0.0%	11 16.9%	0 0.0%	100% 0.0%
	LLLG	0 0.0%	0 0.0%	0 0.0%	2 3.1%	12 18.5%	85.7% 14.3%
	Percentage	100% 0.0%	92.3% 7.7%	100% 0.0%	84.6% 15.4%	92.3% 7.7%	93.8% 6.2%
		LG fault	LL	LLG	LLL	LLLG	Percentage
		Target Class					

Fig 12.4. Overall confusion matrix.

Figure 12.4. shows the overall confusion matrix with 84.8% as overall efficiency. LG, LL, LLG, LLL, LLLG faults have been tested with an efficiency of 88.9%, 83.3%, 75.0%, 80% respectively.

Fig 12.1 is a plot of training confusion matrix. where 75% of data is for training purpose, the matrix has the efficiency of 100%. Fig 12.2 and 12.3 is a plot of testing and validation confusion matrix with an efficiency of 84.8% and 86.4% respectively. While Figure 12.4 shows the overall confusion matrix of 93.8% which is able to classify the fault correctly in the dark grey box and 6.2% of fault misclassified. The green box indicates the number of fault types have been correctly classified and the red box indicates the number of fault types have been wrongly classified. Overall, the results of the fault classification give a satisfactory performance.



CHAPTER 13
CONCLUSION

CONCLUSION

The Work presented in this project provides a technique for transmission line fault classification. Technique is based on S transform and ANN. With the Simulation of "TWO BUS TEST SYSTEM" normal and faulty condition in PSCAD and further analysis in MATLAB. The following conclusions were recorded.

- Fault Index is calculated from S-Matrix for transmission line faults (like LG, LL, LLG, LLL and LLLG).
- Energies are calculated from S-Matrix of current signals, classified LG, LL, LLG, LLL and LLLG type of faults on transmission line accurately

The proposed classification rule in this project gives same results at different fault inception angles. The results obtained shows this method is capable of detecting and classifying different types of faults on transmission line along with the affected phases.

Future Scope:

The work presented in this project is detection and classification of various types of faults (like LG, LL, LLG, LLL and LLLG). using S transform and ANN. The further study can be carried out using ELM (Extreme learning method)

REFERENCES

REFERENCES

- [1] Rafael Arranz, Angel Paredes, Alejandro Rodríguez , Francisco Muñoz,” Fault location in Transmission System based on Transient Recovery Voltage using Stockwell transform and Artificial Neural Networks”,*Electrical power research*, Elsevier, 2021,pp.1-12
- [2] H.A. Jimenez, D. Guillen, R. Tapia-Olvera, G. Escobar, F. Beltran-Carbajal, An improved algorithm for fault detection and location in multi-terminal transmission lines based on wavelet correlation modes, *Electr. Power Syst. Res Elsevier*,2021 pp.192-201
- [3] Seongmin Heo and Jay H. Lee, “Fault detection and classification using artificial neural networks”, *IFAC Conference*, Elsevier, 2018, pp.470-475
- [4] Mohammad Javad Dehghani,” Comparison of S-transform and Wavelet Transform in Power Quality Analysis “, *International Journal of Electrical and Computer Engineering*, ResearchGate, 2009.pp 15-30
- [5] M. Jayabharata Reddy, D.K. Mohanta,” A wavelet-fuzzy combined approach for classification and location of transmission line faults”, *Electrical Power and Energy System Elsevier*, 2007 pp.669–678
- [6] R. N. Mahanty, P. B. Dutta Gupta,” Comparison of Fault Classification Methods Based on Wavelet Analysis and ANN”,*Electric Power Component and System* ,2006 pp.47-60
- [7] D. Das, N.K. Singh, and A.K.Sinha.,” A Comparison of Fourier Transform and Wavelet Transform Methods for Detection and Classification of Faults on Transmission Lines.”,*IEEE*.2006 pp 25-35
- [8] I. W. C. Lee, P. K. Dash.,” S-Transform-Based Intelligent System for Classification of Power Quality Disturbance Signals”, *IEEE Transactions on Industrial Electronics*. IEEE,2003 pp 5-30
- [9] Deyun Wei, Yijie Zhang. “Fractional Stockwell transform: Theory and applications *Digital Signal Processing*” Elsevier, (2021) pp.115
- [10] I. Daubechies, “the wavelet transforms, time-frequency localization and signal analysis”, *IEEE* (1990) pp. 19-28

- [11] Anup Kumar, Himanshu Sharma, Ram Niwash Mahia, Om Prakash Mahela and Baseem Khan, "Design and Implementation of Hybrid Transmission Line Protection Scheme Using Signal Processing Techniques" Hindawi, 2022, pp. 4-18
- [12] K. Chen, C. Huang, and J. He, "Fault Detection, Classification and Location for Transmission Lines and Distribution Systems: a review on the methods," High Volt, IET, 2016. pp. 25–33.
- [13] Santosh K. Padhy, Basanta K. Panigrahi, Prakash K. Ray "Classification of Faults in a Transmission Line Using Artificial Neural Network" , International Conference on Information Technology, ResearchGate, 2018 pp 1-5
- [14] M. Hessine, H. Jouini and S. Chebbi, "Neural Network Approach to Fault Location for High-Speed Protective Relaying of Transmission Lines", Springer International Publishing Switzerland, 2015. pp 5-30
- [15] Banu, G., Suja, S, "ANN Based Fault Location Technique Using one end Data for UHV Lines", Eur. J. Sci. Hindawi 2014. pp. 55
- [16] H. Shu, Q. Wu, X. Wang, X. Tian, "Fault Phase Selection and Distance Location Based on ANN and S-Transform for a Transmission Line in Triangle Network" Proceedings of the 3rd International Congress on Image and Signal Processing. 2010, pp. 3217–3219.
- [17] Ali Raza, Abdeldjabar Benrabah., "A Review of Fault Diagnosing Methods in Power Transmission Systems", Applied science, 2020 pp 2-20
- [18] S. B. Ayyagari, "Artificial Neural Network Based Fault Location for Transmission line," ResearchGate , 2011 pp 55-90
- [19] Ali Raza, Abdeldjabar Benrabah "A Review of Fault Diagnosing Methods in Power Transmission Systems" Applied Science , 2020, pp 5-15
- [20] N. Roy, K. Bhattacharya, "Identification and Classification of Fault Using S-Transform in an Unbalanced Network" IEEE, 2013 pp 5-18
- [21] R.G. Stockwell "A Basis for Efficient Representation of the S-Transform" Elsevier, 2007 pp 10-15
- [22] Sheesh Ram Ola, Amit Saraswat "A Technique Using Stockwell Transform Based Median for Detection of Power System Faults" IEEE, 2018 pp 2-5

BOOKS

- [1] Sunil.S.Rao, "Switchgear Protection Power System", Thirteenth Edition by Khanna Publishers.
- [2] G W Stagg and A H El Abiad "Computer Methods in Power System Analysis" Second Edition by AH wheeler & co private ltd Publishers.
- [3] Prabha Kundur "Power System Stability and Control", Second Edition by McGraw-Hill Education Publishers.
- [4] John G. Proakis "Digital signal processing " 3rd edition by Northeastern University. Dimitris G. Manolakis.
- [5] I.J Nagrath and D.P.Kothari "power system Engineering " 3rd edition by MC Graw Hill

Website

- [1]www.ieeexplore.ieee.org
- [2]www.pscad.com
- [3]www.mathworks.com

APPENDIX

APPENDIX

System Parameter

Parameter for Two Bus System.

Parameters	Generator-1	Generator-2
Base MVA	100 MVA	100 MVA
Base kV	500 kV	500 kV
Base Frequency (Hz)	60 Hz	60 Hz
Rated voltage (kV)	500 kV	500 kV
Rated phase angle(°)	20 °	0 °
Positive sequence impedance (Ω)	48.640 Ω	48.034 Ω
Positive sequence phase angle (°)	69.395 °	71.413 °

Table: Generator Parameters [11]

Bus Voltages:

Bus Number	Rated Voltage (kV)
1	500
2	500

Table: Bus Voltages [11]

Transmission Line Parameters:

Parameters	Transmission line (section1)	Transmission line (Section 2)
Transmission Line length(km)	110 km	110 km
Positive sequence resistance (R1) (Ω/m)	2.4915 Ω/m	2.4915 Ω/m
Positive sequence impedance reactance (X_{11}) (Ω/m)	58.915 Ω/m	58.915 Ω/m

Positive sequence impedance capacitance (X_{c1}) ($M\Omega^*m$)	0.0003405 $M\Omega^*m$	0.0003405 $M\Omega^*m$
Zero sequence resistance (R_0) (Ω/m)	6.341 Ω/m	6.341 Ω/m
Zero sequence impedance reactance (X_{l0}) (Ω/m)	132.098 Ω/m	132.098 Ω/m
Zero sequence impedance capacitance (X_{c0}) ($M\Omega^*m$)	454.955 $M\Omega^*m$	454.955 $M\Omega^*m$

Table: Transmission Line Parameters [11]